Eco-Environment & Health 1 (2022) 86–104

Contents lists available at ScienceDirect

Eco-Environment & Health

journal homepage: www.journals.elsevier.com/eco-environment-and-health

Review

Recent advances in waste-derived functional materials for wastewater remediation

Zhijie Chen [a], Wei Wei [a], Hong Chen [b], Bing-Jie Ni [a,*]

[a] Center for Technology in Water and Wastewater, School of Civil and Environmental Engineering, University of Technology Sydney, NSW, 2007, Australia
[b] State Environmental Protection Key Laboratory of Integrated Surface Water-Groundwater Pollution Control, Shenzhen Key Laboratory of Interfacial Science and Engineering of Materials, School of Environmental Science and Engineering, Southern University of Science and Technology, Shenzhen 518055, China

ARTICLE INFO

Keywords:
Wastewater remediation
Solid wastes
Waste-derived materials
Adsorption
Advanced oxidation processes
Catalytic degradation

ABSTRACT

Water pollution is a major concern for public health and a sustainable future. It is urgent to purify wastewater with effective methods to ensure a clean water supply. Most wastewater remediation techniques rely heavily on functional materials, and cost-effective materials are thus highly favorable. Of great environmental and economic significance, developing waste-derived materials for wastewater remediation has undergone explosive growth recently. Herein, the applications of waste (e.g., biowastes, electronic wastes, and industrial wastes)-derived materials for wastewater purification are comprehensively reviewed. Sophisticated strategies for turning wastes into functional materials are firstly summarized, including pyrolysis and combustion, hydrothermal synthesis, sol–gel method, co-precipitation, and ball milling. Moreover, critical experimental parameters within different design strategies are discussed. Afterward, recent applications of waste-derived functional materials in adsorption, photocatalytic degradation, electrochemical treatment, and advanced oxidation processes (AOPs) are analyzed. We mainly focus on the development of efficient functional materials via regulating the internal and external characteristics of waste-derived materials, and the material's property-performance correlation is also emphasized. Finally, the key future perspectives in the field of waste-derived materials-driven water remediation are highlighted.

1. Introduction

Ensuring clean water is a high-priority issue in the sustainable development of our society. Currently, rapid industrialization and urbanization have led to severe water pollution, which puts much pressure on the ecosystem and human health [1,2]. In this context, eliminating hazardous pollutants (e.g., heavy metals, microplastics, antibiotics, and viruses) from water is of great urgency, which has attracted enormous scientific attention. Thus, efficiently innovative methods have been developed for wastewater remediation, including adsorption, photocatalysis degradation, electrochemical treatment, and AOPs [3–5]. Although these methods differ greatly in mechanisms and operation processes, all of them require functional micro/nanomaterials to attain good pollutant degradation/removal performance. Therefore, designing advanced materials (e.g., carbon materials, metal oxides, and metal sulfides) for the aforementioned methods plays a central role in water remediation [6,7].

Creating functional materials from waste via effective strategies gains increasing attention. The "waste-to-value" principle is of great economic and environmental significance [8,9]. Recently, numerous earth-abundant carbon- and transition metal-based materials designed from wastes have exhibited satisfactory performance in water purification. In this framework, problematic municipal solid wastes are transformed into favorable materials for water remediation via feasible strategies (e.g., pyrolysis, precipitation, and ball milling) [10–12]. To date, diverse biomass wastes (e.g., soya waste [13], lotus seedpod [14], tea waste [15], animal feces [16]), industrial wastes (e.g., coal mining waste [17], red mud [18], sewage sludge [19], brick waste [20]), and electronic wastes (e.g., waste printed circuit boards–WPCBs) [21], spent batteries [22], waste liquid crystal displays [23], electronic packaging waste [24]) with diverse sizes, densities, chemical compositions, shapes, and moistures (Fig. 1a) have been converted into functional materials (e.g., adsorbents, photocatalysts, electrocatalysts) for wastewater purification (Fig. 1b) [25–35]. For example, Liu et al. synthesized biochar

* Corresponding author.
E-mail: bingjieni@gmail.com (B.-J. Ni).

https://doi.org/10.1016/j.eehl.2022.05.001
Received 13 February 2022; Received in revised form 28 April 2022; Accepted 8 May 2022
Available online 22 June 2022

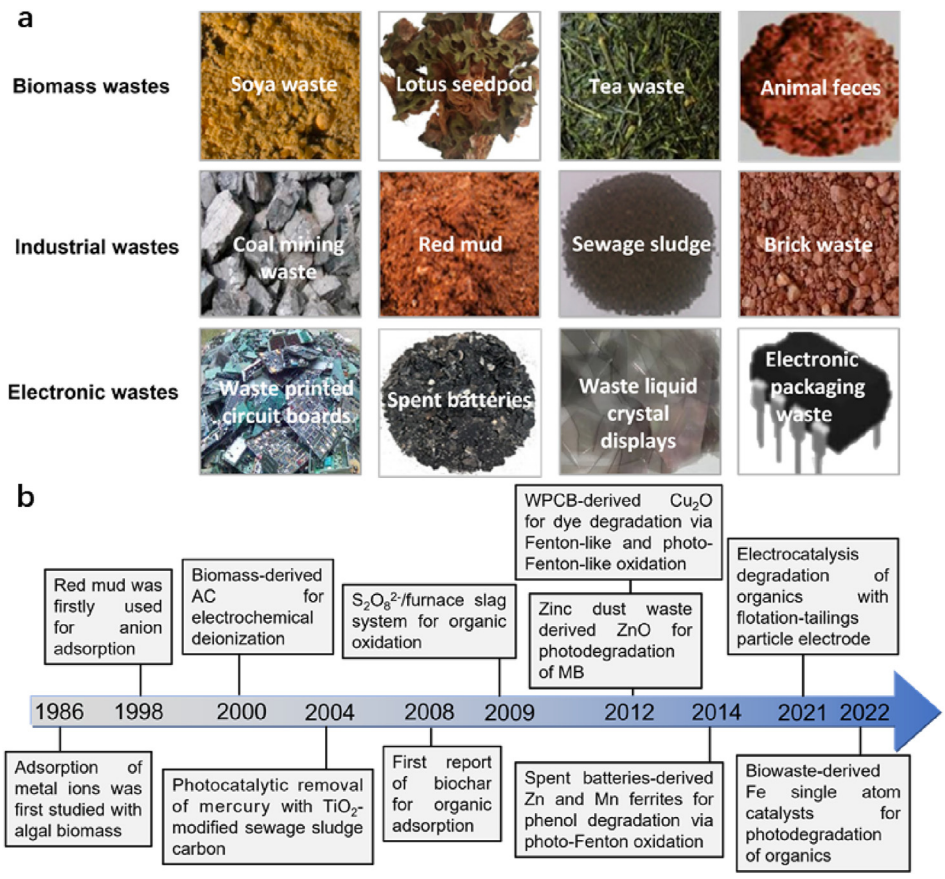

Fig. 1. (a) Representative wastes that have been converted into functional materials for wastewater treatment (Soya waste [13], Copyright © 2021, Elsevier; lotus seedpod [14], Copyright © 2020, Elsevier; tea waste [15], Copyright © 2020, Elsevier; animal feces [16], Copyright © 2020, Elsevier; coal mining waste [17], Copyright © 2021, Elsevier; red mud [18], Copyright © 2021, Elsevier; sewage sludge [19], Copyright © 2022, Elsevier; brick waste [20], Copyright © 2021, MDPI; waste printed circuit boards (WPCBs) [21], Copyright © 2013, American Chemical Society; spent batteries [22], Copyright © 2021, American Chemical Society; waste liquid crystal displays [23], Copyright © 2019, Elsevier; electronic packaging waste [24], Copyright © 2022, Elsevier). (b) Milestone timeline of studies related to the waste-derived materials for wastewater treatment (AC, activated carbon; MB, methylene blue) [25–35].

from agricultural wastes via a pyrolysis process, which presented a high adsorption capacity of 49.70 mg/g toward Pb^{2+} [36]. The "waste-to-value" principle is of great environmental and economic significance because it can significantly minimize the environmental impact of solid/liquid wastes and cut the fabrication cost of functional materials (e.g., adsorbents, catalysts) [37–40]. Apart from adsorption, waste-derived functional materials have also been widely employed in photocatalysis, electrochemical treatment, and AOPs for water purification [41–44]. A critical issue in enhancing the performance of waste-derived materials is the rational design of their nanostructures/components, which can be achieved by controlling the precursors and experimental parameters in the synthesis process. Therefore, developing efficient strategies to turn solid wastes into functional materials with desirable characteristics (e.g., large surface area and high stability) is highly needed. Encouragingly, many sophisticated methods (e.g., pyrolysis, combustion, wet-chemical process, and ball milling) can successfully convert various solid wastes into functional materials, and the selection of synthesis methods highly depends on the properties of waste precursors. For instance, biomass wastes and sewage sludges are often pyrolyzed to obtain carbon materials [45,46], and metal oxides are generally prepared by combustion and sol–gel methods [42,47].

Although a handful of review papers have summarized environmental applications of waste-derived materials, they mainly focused on the utilization of biomass waste-derived biochar in adsorption and AOPs [6,10,12,44–46,48–53]. The systematic summary of the rapidly growing applications of various wastes (e.g., biomass, industrial wastes, and electronic wastes)-derived materials in adsorption, photocatalytic degradation, electrochemical treatment, and AOPs have been seldom reported. Thus, it is urgent to comprehensively review the advances in waste-derived low-cost materials for wastewater remediation.

This review aims to provide an overview of recent advances in the applications of waste-derived materials for wastewater remediation. First, efficient strategies for converting wastes into advanced materials are summarized, and critical experimental parameters within different design strategies are also discussed. Then, recent applications of waste-derived materials in adsorption, photocatalysis, electrochemical treatment, and AOPs are analyzed, and the design of efficient functional materials via regulating the internal and external characteristics of waste-derived materials is emphasized. Finally, perspectives on the development of next-generation waste-derived materials are proposed.

2. Strategies for converting wastes into functional materials

Wastes themselves are rarely used for wastewater purification directly, requiring efficient methods to transform them into desirable functional materials. Currently, diverse biomass, electronic wastes, and industrial wastes with different sizes, densities, chemical compositions, shapes, and moistures have been transformed into functional materials for wastewater treatment. Pyrolysis and calcination, hydrothermal synthesis, sol–gel method, coprecipitation, and ball milling are the mainstream strategies detailed in this section. Moreover, critical experimental parameters that influence the properties of waste-derived materials are analyzed.

2.1. Pyrolysis and calcination

Pyrolysis and calcination are two widely employed thermal activation strategies to convert wastes into functional materials. Pyrolysis is a thermochemical decomposition process generally performed in an inert atmosphere that induces the generation of carbon-enriched biochar, hydrocarbons (bio-oils), and volatile gasses [45,46]. With a different atmosphere in the thermal process, calcination refers to heating solid wastes (e.g., electronic wastes, eggshells) under a high temperature and in an oxygen-involved condition, and it is usually employed to

synthesize metal oxide-based functional materials (e.g., photocatalysts) from wastes [54,55].

The physicochemical properties and yields of pyrolysis products largely depend on the characteristics of starting biomass wastes and the operational conditions of the pyrolysis process (e.g., pyrolysis temperature, heating rate, and residence time) [45,49]. For diverse applications, different physicochemical properties are required; thus, the optimal pyrolysis conditions of biochar are different. Take the pyrolysis temperature as an example, which governs the chemical compositions and surface properties of biochar. It has been well demonstrated that the functional groups (e.g., –OH, –COOH, and –C═O) on the biochar surface are important for the removal of pollutants from wastewater. At high pyrolysis temperatures (e.g., ≥800 °C), the oxygen-containing functional groups on biochar can be well obliterated to shape aromatic structures with higher carbonization degrees. In this context, the high-temperature-derived biochar owns high hydrophobicity and aromaticity and often contributes to excellent adsorption performance toward organic contaminants [56]. Nevertheless, a higher temperature could also lead to the chemical rearrangement of biochar. The destruction of the biochar structure would obstruct the pores, thus degrading the adsorption performance of biochar [57]. Differently, biochar prepared at a relatively low pyrolysis temperature (e.g., ≤450 °C) contains richer surface functional groups than that synthesized at high temperatures. These functional groups can provide abundant active sites for the adsorption of inorganic pollutants and the activation of persulfate (PS) and H_2O_2 [58]. However, another study suggested that compared with the rich oxygen function groups and persistent free radicals (PFRs) of biochar pyrolyzed at low temperature (e.g., 300 °C), the graphite electron donor–transfer complex generated during pyrolysis of biochar at higher temperature (e.g., 700 °C) played a more important role in the activation of PS, which acted as electron donor, increased electron transfer and formed graphite holes during the degradation of acid orange 7 [59]. In this context, the pyrolysis of biochar should be checked on a one-by-one basis to optimize its surface chemistry (functional groups, defects, hydrophility), conductivity, and nanostructure (porosity) for target applications.

A critical issue involved in the pyrolysis of biochar with a relatively low temperature is the formation of hazardous environmentally persistent free radicals (EPFRs, e.g., oxygen-centered, carbon-centered, and oxygenated carbon-centered radicals), which may have potentially adverse effects on the ecosystems and host organisms [60]. Accordingly, toxicological studies should be implemented in the production and adoption stages of biochar to determine the specific risks to the surrounding living organisms concerning generated EPFRs in biochar [61]. In addition, it is necessary to optimize the pyrolysis parameters and the biomass properties to limit the generation of EPFRs [62]. Apart from pyrolysis temperature, the heating rate is another widely studied parameter. Depending on the heating rate and residence time, the pyrolysis process can be divided into slow pyrolysis, fast pyrolysis, and flash pyrolysis. The heating rate has a big influence on the contents of gaseous, liquid, and solid products [12,49]. Generally, biochar synthesized directly from biomass pyrolysis shows poor surface functionality, low porosity, and small surface area, which profoundly confine its applications in wastewater treatment. The surface modification and functionalization of biochar (e.g., alkaline/acid modification, chloride modification, loading of functional nanomaterials, surface doping) have been extensively studied to address this issue, and shape the nanostructure, chemical composition, electronic structure, and stability of biochar-based materials for typical applications [12].

In the calcination procedure, the calcination temperature influences the nanostructure and crystallinity of waste-derived materials, and thus, their performance. In general, a higher temperature leads to a higher crystallinity and a more severe aggregation of particles [63,64]. The former can influence the electronic structure of materials, and the latter will result in a reduced surface area [65]. In this term, the optimal calcination temperature should be checked on a case-by-case basis for different wastes. Controlling the chemical composition of waste precursors is another route to enhance the performance of waste-derived materials [42]. This can be achieved by calcinating the mixture of wastes and desirable chemicals or wastes [66,67]. For example, Xu and coworkers developed a Fe_2O_3-TiO_2/spent fluid catalytic cracking catalyst composite (Fe-Ti/SF) via an impregnation-calcination process [68]. Benefiting from the favorable photoactivity of Fe_2O_3 and TiO_2, the interparticle electrons transfer between TiO_2 and Fe_2O_3, and the fast charge transfer rate, the Fe-Ti/SF displayed a higher methylene blue (MB) photodegradation efficiency over its single Fe_2O_3 and TiO_2 loaded counterparts. With the one-pot calcination process, one can optimize the chemical composition of waste-derived materials by adding suitable precursors to wastes.

2.2. Hydrothermal synthesis

Hydrothermal synthesis involves chemical reactions in water solution at both high temperature and pressure in sealed, high-pressure vessels. There are mainly two routes to construct functional materials from wastes via the hydrothermal method. First, the hydrothermal carbonization of biomass can produce hydrochar, which also holds great potential in wastewater remediation [69,70]. Of particular interest, this method is suitable for the conversion of biomass wastes with high moisture content (e.g., sewage sludge and animal excreta) because it avoids the separate drying process [71]. Second, hydrothermal synthesis can be applied to the preparation of metal-based functional materials/composites from solid/liquid wastes, such as metal oxides and sulfides [72–76], metal oxide/sulfide composites [77], metal (hydr) oxide/carbon composites [78], metal sulfide/biochar composites [79], and red mud/biomass waste composites [80]. The reaction temperature, solid/liquid ratio, pH value, and reaction time of the hydrothermal process are important factors that influence the properties (e.g., nanostructure, phase, and surface property) of waste-derived materials.

Aside from the single hydrothermal process, many studies have attempted integrated techniques to design efficient functional materials from waste. As reported, a hydrothermal synthesis (210 °C, 12 h) followed by one-step calcination (750 °C, 1 h) was used to construct hierarchical activated porous carbon microspheres from fallen *Platanus orientalis* leaves [81]. Similarly, an integrated hydrothermal process-thermal conversion method was applied to convert red mud into porous γ-Al_2O_3 microspheres [82]. For the hazard-free treatment and resource utilization of wastewater sludge, Cai et al. developed a coagulation-hydrothermal reaction-pyrolysis technique to turn waste sludge into mesoporous biochar composed of goethite, quartz, biochar, and polymer [83]. Of note, the combination of these methods can efficiently convert diverse wastes (e.g., plant leaves, sludge, red mud) into value-added materials.

2.3. Sol–gel method

The sol–gel method proposes the chemical transformation of a liquid "sol" (generally a colloidal suspension of inorganic particles) into a gelatinous network "gel" phase with a subsequent high-temperature calcination process and further conversion into oxide materials [84]. The obtained materials keep high crystallinity, purity, homogeneity, as well as high modifiability [85]. The main operational conditions of the sol–gel process contain solution concentration, reaction time, temperature, and pH value. Currently, a series of wastes have been exploited to fabricate functional materials via the sol–gel process [86–90]. The mainstream method converts solid wastes (e.g., electronic wastes and biomass) into liquid wastes, which act as the sol's precursor [87,88]. For example, the spent Ni–Cd batteries' positive-electrode leaching solution was transformed into mixed oxide containing iron, nickel, cobalt, and cadmium via the sol–gel method, and the metal oxide exhibited high photocatalytic degradation performance toward the textile-reactive black V–2B dye [91]. Another method refers to the preparation of

waste-bearing composite materials via the sol–gel process. In this framework, small-sized solid wastes (e.g., fly ash) can be directly added to the reaction solution and act as a support for functional components, and the resulting composites can be applied in wastewater purification [86]. As reported, the TiO_2/calcined eggshell composite was prepared by a sol–gel technique followed by a self-assembly coprecipitation method, which acted as a hybrid nano-biosorbent for the removal of acid dye from aqueous media [92]. Differently, Zhang et al. developed a sol–gel/pyrolyzing route to construct the magnetic biochar-$MnFe_2O_4$ nanocomposite. Within the composite, biochar could support and disperse $MnFe_2O_4$ effectively, which contributed to the superior adsorption performance [93].

2.4. Coprecipitation

Coprecipitation is a convenient way to prepare oxide-based nanomaterials, which can be defined as the occurrence of simultaneous nucleation, growth, coarsening, and/or agglomeration processes in solution [94]. The properties of the obtained precipitates, such as composition, size, and morphology, highly depend on the reaction parameters (e.g., precursor ratio, temperature, pH value, surface ligand, etc.). Similar to the sol–gel process, there are mainly two strategies for constructing functional materials from wastes with the coprecipitation process: (1) extracting metal components from solid wastes (e.g., electronic wastes) to liquid phases, which work as the precursor of metal oxides in the coprecipitation process [95,96]; (2) focusing on applying waste-derived carbon materials as the support of metal (hydr)oxides, and producing metal (hydr)oxides/carbon composites with the coprecipitation method [97–100]. For instance, a chemical coprecipitation and subsequent pyrolysis process were implemented to prepare magnetic reed biochar in which iron oxides were loaded on the surface of biochar [101]. A similar impregnation-pyrolysis technique was used to develop iron-modified biochar for phosphate adsorption starting from waste-activated sludge. Noticeably, the iron in $FeCl_3$-impregnated sludge-based biochar mainly existed in the amorphous phase, which improved the adsorption performance [102].

2.5. Ball milling

Ball milling, also known as mechanochemical milling, is a mechanical-chemical process that consumes mechanical energy to cause structural and chemical changes in materials [5,103]. Compared with traditional material synthesis methods (e.g., hydrothermal process, calcination, and pyrolysis), the mechanochemical process owns many advantages: (1) avoiding the energy-consuming high-temperature operation, (2) reducing the time and chemicals required in the milling process, (3) facilitating large-scale fabrication of materials with high yield from wastes [104,105]. In addition, depending on the requirement of products, one can select suitable milling parameters such as milling time, temperature, speed, atmosphere, and ball/material ratio.

Ball milling has been widely employed in preparing functional materials from solid wastes, with biochar-based materials as the representative [10]. A main function of milling is to decrease the size of materials, resulting in enlarged surface area and thus benefits the reaction between materials and pollutants [106]. By using ball milling to reduce the size of waste cassava slag, the following hydrothermal carbonization could turn the milled slag into cassava slag biochar for dye adsorption [107]. Incorporating nano-sized functional materials in highly porous and structurally stable biochar via ball milling produces nanocomposites that consolidate the advantages of both raw materials for wastewater remediation [10,108]. For example, a pyrolysis-ball milling technique was capable of synthesizing magnetic biochar based on biomass and iron or iron oxides [109]. Apart from reducing the size of wastes, the introduced intensive mechanical energy can also activate wastes by increasing the number of surface functional groups and defects [110]. Therefore, ball milling is suitable for converting solid wastes into targeted functional materials (e.g., nanostructure and surface chemistry).

3. Waste-derived adsorbents for pollutant removal

Adsorption is a cost-effective method to remove pollutants from wastewater [36,111,112]. The adsorption efficiency highly depends on the properties of adsorbents, especially the surface area and surface functional group. Waste-derived low-cost materials with flexible physical and chemical properties have gained great interest in the adsorption of metal/anion ions, dye, and antibiotics, as summarized in Table 1.

3.1. Inorganic pollutants

Inorganic ions in wastewater are of growing environmental concern due to their high toxicity and cumulative biological effects [112,115,131]. Rich in hydroxyl, carboxyl, and other functional groups, waste-derived materials can react with inorganic ions via ion exchange, surface complexation, hydrogen bonding, π-π interaction, electrostatic attraction, etc [45]. Therefore, they can be employed as competent adsorbents to remove inorganic ions.

Biowaste-derived carbon materials (e.g., AC) are widely used absorbents for heavy metal ions mainly due to their rich oxygen-based functional groups (e.g. –OH, –COOH, and –C═O), high surface area, and low price [132]. For enhancing the adsorption performance of biowaste-based adsorbents, nanostructure regulation and surface modification via acid, base, oxidizing agent, organic compound, and salt activation have been widely explored. Typically, base (KOH, NaOH) and chloride ($ZnCl_2$) activation in the pyrolysis process can optimize the porosity of the activated biochar, which benefits the adsorption of inorganic ions via increasing the surface area and facilitating mass/charge transfer. Differently, acid (e.g., H_2SO_4) treatment mainly focuses on introducing functional groups (e.g., $–SO_3H$), which can attract metal ions efficiently and improve the adsorption capacity [133]. Similarly, the application of oxidizing agent (e.g., NaClO) will increase the number of active binding sites by oxidizing some of the functional groups of biochar to carboxylic groups; hence, more metal ions can be adsorbed and removed [134].

Anions (e.g., F^-, Cl^-, NO_3^-, SO_4^{2-}, and PO_4^{3-}) can also be removed by waste-derived carbon materials via adsorption. Positively charged segments should be introduced onto the carbon surface to ensure a high removal efficiency. Thus, chemical modifications are required to obtain desirable functional groups (e.g., amidine and amino groups) and multivalent metal ions [135]. For N-containing group modification, Pan and coworkers developed a recoverable amine-functionalized biosorbent (BR-N) from biogas residue for NO_3^- and PO_4^{3-} removal from wastewater [136]. The BR-N showed a cross-staggered structure with rich quaternary-amine groups. These characteristics led to enhanced pollutant diffusion and strong electrostatic attraction of BR-N with NO_3^-/PO_4^{3-}. In terms of metal ion regulation, Yang et al. found that the adsorption performance of PO_4^{3-} on Fe-modified biochar derived from waste-activated sludge was better than the untreated counterparts [102]. The Fe species in the biochar existed mainly as amorphous hematite and hydroxides, which enhanced the PO_4^{3-} adsorption. In addition, ligand exchange played a critical role in the adsorption of PO_4^{3-} by the Fe-modified biochar.

Beyond biowaste-based materials, industrial wastes (e.g., slag, mine waste, spent limestone, fly ash, and electronic waste)-derived adsorbents also exhibit good performance for inorganic ion removal [22,137–140]. Adsorbents derived from industrial wastes are generally in the form of (mixed) metal (hydr)oxides, which possess abundant active sites for the adsorption of metal ions and anions. Apart from the advantages in chemical composition, the nanostructure of some industrial waste-derived adsorbents also enhances the adsorption performance. Zou et al. developed a zeolite from the spent $LiFePO_4$ battery via hydrothermal treatment, which held three-dimensional 12-member-ring channels [22]. Benefiting from its high structural porosity, high chemical adsorption capacity, and fast cation exchange, the waste-derived zeolite showed a high Pb^{2+} removal capacity of up to 723.8 mg/g. It

Table 1
Summary of representative waste-derived adsorbents for pollutant removal.

Adsorbent	Pollutant	Adsorption conditions					Adsorption amount (mg/g)
		A.D.[a] (g/L)	C_0[b] (mg/L)	Time (h)	pH	T[c] (°C)	
WPCB-derived adsorbent	Cd(II)	1	562	4 days	4	20	236.12 [113]
Corn stalk-derived biochar	Pb(II)	2	100	12	5.5	25	49.7 [114]
Leaching residues of biotite minerals	Hg(II)	–	200	2	2	25	355.23 [115]
Sorghum root-derived AC[d]	Pb(II)	0.2	40	1	–	–	197.6 [116]
Cow dung waste-derived composite (PEI-Fe_3O_4@CDB)	Cu(II)	5	1200	3	7	25	183.82 [117]
	Cd(II)	5	1200	3	7	25	231.48 [117]
Blast furnace slag-derived Al_2O_3-SiO_2-BFS	U(VI)	0.5	300	5	6	25	88.5 [118]
Pinewood-derived biochar	NO_3^-	2.5	60	6	2	22 ± 1	4.2 [119]
	PO_4^{3-}	2.5	60	6	2	22 ± 1	20.5 [119]
Red mud/base treated rice husk composite	SO_4^{2-}	7.5	100	1.5	4	65	12.41 [80]
Paper waste-derived AC	F^-	0.3	12	18	5	25	39.76 [120]
Acidosasa edulis shoot shell-derived biochar	ReO_4^-	3	20	8	1	~22	4.42 [121]
Pine sawdust-derived AC (CZn5)	Basic Green 4	5	50–2000	2	6–10	26	370.37 [122]
Rice husk-derived AC (PK-AC)	RhB[e]	10	300	3	1.3–10.2	19.8	235 [123]
Blast furnace sludge-derived carbonaceous adsorbent	Basic Orange 2	1	124.36	2	6.5–7.5	25	10.1 [124]
Sugarcane bagasse derived biochar/ZnO	Reactive Red 24	1	250	1	3	RT[f]	105.24 [125]
Sewage sludge-derived AC	Amoxicillin	2.5	100	–	6	–	27 [126]
Polyethylene terephthalate waste-derived α-Fe/Fe_3C	Tetracycline hydrochloride	0.25	200	1.5	6	25	652.08 [127]
Modified waste expanded polystyrene	Fluoroquinolone	0.2	25	0.5	6	–	554.3 [128]
Walnut shell-derived AC	SMX[g]	0.01	40	48	5.5	30	93.5 [129]
	Metronidazole	0.01	40	48	8	30	107.4 [129]
Methanol-modified biochar	Tetracycline	1	100	12	5	30	95.63 [130]

[a] Adsorbent dosage.
[b] Initial pollutant concentration.
[c] Temperature.
[d] Activated carbon.
[e] Rhodamine B.
[f] Room temperature.
[g] Sulfamethoxazole.

should be noted that the adsorption of ions on waste-derived oxides highly depends on the reaction conditions, including pH value, reaction time, and temperature. As suggested by Qiu and coauthors, the adsorption behavior of Cd^{2+} by the hydrothermally modified circulating fluidized bed fly ash (HM-CFB-FA) was controlled by the initial pH value. When the initial pH value was <6.2, the chemical precipitation process was inhibited by H^+, and the adsorption function dominated in the removal of Cd^{2+}. Differently, when an initial pH > 6.2 was adopted, part of the oxides of Ca and Al might undergo hydrolysis and ionization reactions. Afterward, the release of OH^- improved the solution pH, which led to the chemical precipitation of Cd^{2+} (Figure S1) [137]. This pH-dependent ion adsorption is a ubiquitous phenomenon, which should attract attention to optimize adsorption performance and uncover the adsorption mechanism. Another interesting issue worth mentioning here is the adsorption time-dependent adsorption mechanism. Recently, Pérez et al. found that the fundamental role of $Ca(OH)_2$ in waste-derived $Ca(OH)_2$/$CaCO_3$ materials for P adsorption finished before 15 min, and thereafter, $CaCO_3$ was responsible for the removal of orthophosphate ions [141]. Under a high concentration of orthophosphate ions, direct ligand exchange of PO_4^{3-} by CO_3^{2-} appeared while improving the crystallinity of the generated apatite.

Combining the merits (e.g., large surface area, low cost, and high adsorption activity) of different adsorbents can form high-performance composites for pollutant removal. Carbon/zeolite-based composites have aroused great interest [142,143]. For instance, Han et al. developed a nanoscale zerovalent iron (nZVI)-loaded microspherical carbon (SC) composites (SCZ) from the waste carton for Cr(VI) ion removal (Fig. 2a). The SC facilitated the adsorption of Cr(VI) ions, which were further reduced to Cr(III) by nZVI and –OH on SC. Simultaneously, the nZVI converted to iron oxides (Fig. 2b) [144]. The SCZ composite integrates adsorption and chemical reduction in one system, which accelerates the removal of hazardous high-valence metal ions. Apart from nZVI, metal (hydr)oxides/sulfides/metal–organic frameworks (MOFs) with high adsorption capacity are

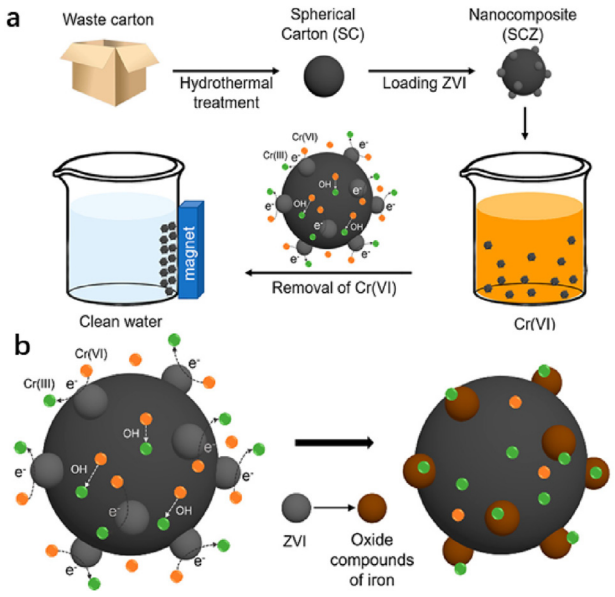

Fig. 2. Waste-derived adsorbents for metal ions removal. (a) Schema of the synthesis of a new nanocomposite (SCZ), spherical carbon (SC) loaded with zerovalent iron (ZVI), and its application in Cr(VI) adsorption. (b) Schematic diagram of Cr(VI) removal mechanism by SCZ [144], Copyright © 2018, American Chemical Society.

widely coupled with carbon/zeolite materials. Ngambia and coauthors designed a sewage sludge-derived biochar (SDBC)-Mg(II) composite via a facile precipitation-calcination process, which was able to eliminate >99% of Ag^+, Pb^{2+}, Cu^{2+}, and Cd^{2+} ions from pond water [145]. The high adsorption performance can be attributed to the high surface area (91.57 m^2/g) and rich sorption sites.

3.2. Organic pollutants

The wide application of dye, herbicides, pesticides, surfactants, plastics, pharmaceuticals/antibiotics, and fungicides in the mining, chemical, food, and light industries causes serious organic pollution and delivers risks to the aquatic environment and human health [146–151]. It is effective to remove those organic pollutants by sorption, and the main removal mechanisms involve electrostatic interactions, hydrogen bonding, ion exchange π-π interactions, n-π interactions, and pore-filling [152,153]. Carbon-based materials are widely studied due to their high surface area and flexible surface chemistry. Using molecular simulations, Bahamon and coworkers found the adsorption properties of AC for five typical antibiotics (naproxen, paracetamol, amoxicillin, diclofenac, and ibuprofen) were different and were essentially associated with their atom affinities and molecular structures [154]. Given the diversity in the structure of organic contaminants, a series of strategies aiming at structural modifications and surface functionalization have been performed on waste-derived carbon materials.

Texture properties and surface chemistry of adsorbents play a central role in determining their adsorption capacity toward organic pollutants. It is widely accepted that adsorbents with a porous structure and high surface area are suitable for the adsorption of organic contaminants [155]. Unlike texture properties, the role of surface functional groups in influencing the adsorption of organic pollutants shows a case-by-case feature. Alivand et al. found that the melamine incorporation (as the agent for mesopore formation) and $–NH_2$ immobilization could enhance the adsorption capacity of asphaltene residue-derived nanoporous carbons (IANC) for amoxicillin and metronidazole antibiotics elimination from wastewater effluents. Apart from the melamine modification-induced high surface area (2693 m^2/g) and mesopore volume (1.61 cm^3/g), the introduction of the $–NH_2$ group significantly improved the adsorption energy of amoxicillin and metronidazole due to a more favorable electrostatic and charge-transfer effects [156]. The water flow characteristics should be optimized to ensure efficient contact between pollutants and functional groups on adsorbents. Guo et al. designed a cross-flow filtration material (β-CD/WS) based on wood sawdust and β-cyclodextrin-polymer. The pharmaceutical contaminant water flowed through the micropores on the surface of the cell walls and the sawn-off vessel channels. The water flow characteristics of β-CD/WS led to full contact between organic pollutants (e.g., propranolol) and grafted β-CD on the cellulose backbone of WS, thus improving the pollutant removal efficiency [157]. It should be noted that not all surface functionalization leads to enhanced adsorption performance. For example, Jaria and coworkers found that the introduction of thiol groups on waste-based AC resulted in a worse adsorption capacity toward SMX [158]. This was because the specific surface area played a more decisive role than the proposed functionalization in the adsorption performance. Similar studies also pointed out that the most influencing factors for the organic pollutants' adsorption were the AC's textural parameters, but not the introduced functional groups [159,160]. Therefore, for surface functionalization, it is necessary to consider the effect of functional groups on the specific surface area and porous properties of adsorbents.

Composites can integrate the merits of different functional materials and thereby show enhanced adsorption performance. Materials like metal oxides, clay minerals, zeolite, silica, and nZVI are promising candidates to enhance the adsorption performance of carbon materials by introducing functional groups and active sites [161–164]. Mei and coworkers developed a Fe-N co-modified biochar (Fe-N-RSBC) via a one-pot pyrolysis process. The Fe-N-RSBC possessed rich functional groups, graphitized carbon structure, and magnetic components (Fe_3O_4, γ-Fe_2O_3, and Fe_3C), which led to a high tetracycline (TC) adsorption ability (156 mg/g). The Fe components decorated porous biochar adsorbed TC via surface complexation, electrostatic interaction, hydrogen–bond interaction, pore filling, and π-π interaction [165]. Of particular interest, low-cost layered clay minerals with large surface areas can not only enlarge the specific surface area but also interact with the pollutants via exchangeable cations in the layer of minerals [163]. Apart from these carbon-based composites, Basaleh et al. developed a steel slag-acrylamide acrylic acid (SSAA) copolymer with an addition polymerization method. The SSAA composite showed great performance in the removal of cationic and anionic dyes, and the maximum efficiencies of 94% and 97% were attained for MB and methyl orange (MO), respectively. Further investigations suggested that physical adsorption was found to be the dominating mechanism for MB, while the chemisorption mechanism was found for MO [166]. Such inorganic/organic composites combining the merits of low cost and high performance are of great interest in the development of efficient multifunctional adsorbents.

4. Waste-derived photocatalysts for pollutants degradation

Photocatalysis is an appealing strategy to exploit green and renewable solar energy for pollutant degradation. When photocatalysts are exposed to appropriate light irradiation, excited holes (h^+) and electrons (e^-) will be generated [167,168]. The photogenerated h^+ with a strong oxidation ability can oxidize pollutants directly, and several important free radicals (e.g., ·OH) generated by the reaction of h^+ and e^- with OH^-, H_2O, and O_2 can also degrade pollutants into small nontoxic or less toxic compounds (e.g., CO_2, H_2O) [169–172]. To enhance the utilization efficiency of sunlight and cut the cost of semiconductor photocatalysts, waste-derived metal oxide/carbon-based materials have attracted great interest. Table 2 summarizes representative waste-derived photocatalysts for pollutant degradation.

4.1. Waste-derived semiconductor photocatalysts

Semiconductor metal oxide-based catalysts are widely implemented in the photodegradation of pollutants. Metal-bearing solid wastes are promising precursors for the fabrication of metal oxide photocatalysts. Abdo et al. found that the recovered SnO_2 nanoparticles from WPCBs leachate solution showed a high photocatalytic performance toward MB dye degradation under UV light illumination [182]. The key to the successful preparation of the high-performance SnO_2 nanoparticles was the selective leaching of Sn from WPCBs in the Na_2-EDTA chelating agent. Eggshell, a ubiquitous biowaste, can be employed to prepare CaO via a calcination process. The obtained CaO nanopowders enable the photodegradation of the textile acid dye Lanasyn Rez F5B [183] and the MB dye [184]. With a bandgap of 2.75 eV, copper slag (mainly containing magnetite and fayalite) could be directly applied in the photooxidation of a series of alcohols and the photoreduction of water [185]. Hence, the copper slag realizes the oxidation of organic pollutants and the simultaneous hydrogen production in industrial wastewater under solar radiation.

Carbon-based metal-free photocatalysts (e.g., carbon dots, graphitic carbon nitride (g-C_3N_4)) obtained from biowastes possess good performance toward pollutant mineralization. As a metal-free and visible light-responsive material, g-C_3N_4 is widely used in the photodegradation process. Yang and coworkers developed a g-C_3N_4 from the mixture of dicyandiamide and mushroom waste via a thermal condensation process followed by thermal exfoliation. The waste-derived photocatalyst exhibited a good activity toward the degradation of MB (over 90% removal in 270 min) due to its high graphitic degree and few pyrrolic-N forming repeated tri-s-triazine units oriented along the plane [186]. Photoactive carbon dots and graphene can also be directly fabricated from biowastes [187–190]. Apart from the photodegradation of dye, carbon dots also enable the photoreduction of Cr(VI). Aggarwal et al. found that carbon dots obtained from cellulose could remove 20 ppm of Cr(VI) completely in wastewater within about 2 h under sunlight illumination [189]. In this context, the applications of carbon dots can realize the co-removal of organic and inorganic pollutants.

The emerging single-atom catalysts (SACs) have gained growing scientific attention due to their ultrahigh atom utilization efficiency and

Table 2
Summary of representative waste-derived photocatalysts for pollutant degradation.

Photocatalyst	Pollutant	Photodegradation conditions					Degradation efficiency (%)
		P.A.[a] (g/L)	C_0 (mg/L)	Irradiation	Time (h)	pH	
Cotton waste-derived carbon microtube	BPA[b]	0.5	10	Visible light	2	–	~95 [173]
Industrial waste-derived TiO_2/Fe_2O_3	Methyl blue	1	79.9	Natural sunlight	2	5	100 [174]
	RhB	1	47.9	Natural sunlight	2	5	93 [174]
	Congo red	1	69.67	Natural sunlight	2	5	99 [174]
Waste toner powder-derived g-C_3N_4-Fe_2O_3	MO	1	20	Natural sunlight	1.5		99 [175]
Spent batteries-derived graphene oxide/copper composite	MB	0.5	100	UV light[c]	3	–	90 [176]
Industrial waste-derived multiphase photocatalysts	Ritonavir	0.4	10	Visible light	0.25	–	95 [177]
	Lopinavir	0.4	10	Visible light	1	–	95 [177]
ZnO immobilized onto wood waste-derived AC	MB	3	10–50	Visible light	3	8	100 [178]
Cd^{2+}-loaded spent adsorbent	MB	0.4	20	Visible light	0.33	–	97.41 [179]
Pb^{2+}-loaded spent adsorbent	Acetaminophen	0.2	5	Visible light	3	7	93 [180]
Polystyrene waste supported Ag-TiO_2	MB	6.7	45	UV light	2.5	6	60 [181]
	Cr(VI)	6.7	15	UV light	2.5	2	32 [181]
Red mud modified montmorillonite	Phenol	1	100	Visible light	1	6	95 [67]
	Cr(VI)	1	60	Visible light	2	4	97 [67]

[a] Photocatalyst amount.
[b] Bisphenol A.
[c] Ultraviolet light.

remarkable catalytic activity [191–193]. Li et al. recently synthesized a Fe single-atom catalyst (FeSAC-800) from iron mines contaminated biomass waste ferns by facile pyrolysis (Fig. 3a) [35]. The FeSAC-800 owned a FeN_4 structure confined in the porous carbon (Fig. 3b). The FeSAC-800 presented a high photodegradation efficiency in the catalytic of typical antibiotics in 60 min. With the addition of peroxymonosulfate (PMS), the photodegradation of norfloxacin (NOR) followed a Fenton-like oxidation route, and ROS (e.g., $O_2^{\cdot-}$, $^1O_2$) played a central

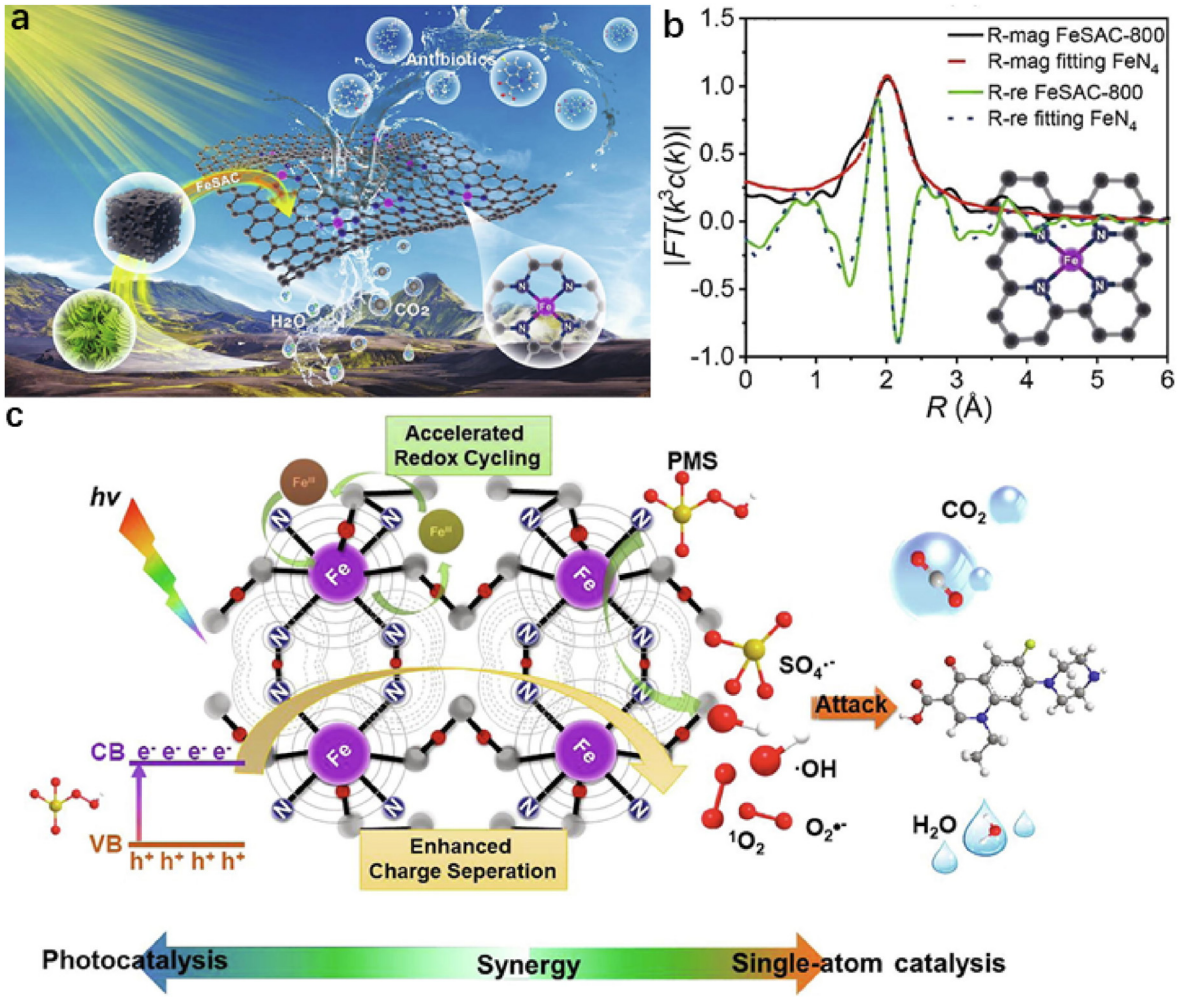

Fig. 3. Waste-derived single-atom catalysts for pollutant photodegradation. (a) Schema of utilizing biomass waste ferns for photocatalytic degradation of antibiotics. (b) Extended X-ray absorption fine structure R-space fitting curve of FeSAC-800. (c) Photocatalytic mineralization mechanism of NOR by waste-derived FeSAC-800 [35], Copyright © 2022, Elsevier.

role (Fig. 3c). Thus, metal-contaminated biomass wastes are appealing precursors for the preparation of cheap and photoactive SACs for wastewater remediation.

4.2. Waste-derived composite photocatalysts

For upgrading the photocatalytic performance of semiconductor photocatalysts, it is highly recommended to design waste-derived composite photocatalysts with low electron–hole recombination efficiency, a wide range of light absorption, strong photo anticorrosion, and high electronic conductivity. Typically, photoactive carbon-based composites are frequently employed to degrade organic pollutants [194,195]. Take the e-waste-derived g-C_3N_4-Fe_2O_3 photocatalyst as an example [175]. Compared with the single g-C_3N_4 and Fe_2O_3, the composite showed better photocatalytic activities for the degradation of MO and textile effluents due to the enhanced absorption of visible light, formation and synergistic effect of heterojunction in g-C_3N_4-Fe_2O_3, and the promoted separation efficiency of photoinduced electron-hole pairs. Another feature of the iron oxide-based composite was that it could be easily separated and recovered from the solution under an external magnetic field. For the graphitic carbon-encapsulated V_2O_5 nanocomposites (GC-V_2O_5) developed via an ultrasonication process (Figure S2a), the enhanced photocatalytic performance toward dye degradation could be attributed to the encapsulation of defective V_2O_5 by the waste-derived conductive carbon that would enhance the photocarrier transport and the catalytic reaction at the interface and in the medium of the dye-catalyst mixture (Figure S2b-c) [196]. Beyond these binary carbon/metal oxide composites, the ZnO-polypyrrole (PPy)-AC-based trinary-nanocomposite also attained a high photodegradation efficiency of 98.12% toward MB dye in 20 min at room temperature under visible light. Therefore, designing multicomponent composites from wastes might improve photocatalytic performance, and an emphasis should be put on figuring out the role of each component in the composites.

Waste biomass-derived biochar-based composites are widely employed for organic and heavy metal photodegradation [197]. Biochar is good support for photoactive materials due to its large surface area, which can effectively upgrade the durability of photocatalysts and shape the morphology of the nanoparticles. What is more, the strong adsorption capacity, rich surface functional groups, and good electrical conductivity of biochar can improve the photocatalytic performance of composite catalysts [198]. Recently, metal oxide/biochar composites have demonstrated high potential in the photodegradation of pollutants. Taking the red mud/g-C_3N_4 (RM-CN) composite as a representative, which was synthesized by a thermal polymerization process (Figure S2d) [199]. Compared with single g-C_3N_4, the specific surface area and the optical absorption and photocurrent response of RM-CN have been significantly enhanced with the presence of red mud. Under the synergistic effect of adsorption and photocatalysis, RM-CN composite exhibited excellent photodegradation performance for dyes and antibiotics. In a tricomponent composite biochar@$CoFe_2O_4$/Ag_3PO_4, Zhai et al. found that the electrical conductivity of biochar enabled to assist the transfer of e^- from the conduction band (CB) of Ag_3PO_4 to the valence band (VB) of $CoFe_2O_4$ and then to the CB of $CoFe_2O_4$, in the Z-scheme biochar@$CoFe_2O_4$/Ag_3PO_4 photocatalyst (MBA-3) [200]. This biochar-mediated electron movement significantly promoted the separation of photogenerated electron–hole pairs, and thus, contributed to the efficient degradation of BPA.

Aside from carbon-based composites, recent attempts have investigated waste-derived metal oxide-based composites for pollutant degradation. By using eggshells as the template and support, Zhang et al. developed a CuS/$CaCO_3$ nanocomposite. Under NIR irradiation, the nanocomposite displayed good photocatalytic performance for 4-nitrophenol reduction (98% removal efficiency in 15 min) and strong photothermal ablation behavior against bacteria [201]. Notably, the waste eggshell not only acted as a support to immobilize nanoparticles but also could provide active carbonate radicals for the degradation of target pollutants. Composites based on earth-abundant mining/industrial wastes, including the mesoporous ZnO@silica fume-derived SiO_2 [202], TiO_2/biogenetic jarosite composite [203], and red mud/montmorillonite [67] show good catalytic performance for the degradation of organic pollutants and the reduction of metal ions. Considering the large-scale production and negative effect of mining/industrial wastes, as well as their oxide–rich properties, it is of great environmental and economic value to design high-performance mining/industrial wastes-based composites with suitable band structures for photodegradation of contaminants.

5. Waste-derived materials for electrochemical wastewater treatment

Electrochemistry-driven wastewater treatment techniques have many advantages, including high efficiency, less chemical consumption, ease of implementation, and environmental friendliness [4,204]. The performance of the electrochemical wastewater treatment system largely depends on the electroactive materials, and designing cost-effective materials is a critical issue. At present, waste-based electroactive materials have displayed great potential in the electrochemical deionization and pollutant electrodegradation processes (Table S1-2), which are discussed in this part.

5.1. Waste-derived materials for electrochemical deionization

Electrochemical deionization is a highly energy-efficient and effective desalting technique to remove ionic elements or salt ions from wastewater/seawater via electrosorption and/or faradaic reactions [205]. Electrochemical deionization properties significantly rely on the electrode materials. High-performance electrodes should meet several textural and electrochemical requirements, including large specific surface area, high ionic conductivity, high porosity, and strong mechanical stability [206]. Recently, biomass and plastic waste-derived carbon materials have been widely employed as promising electrodes for electrochemical deionization [207]. Great efforts have been made to engineer porous structures within carbon materials to enhance the deionization performance. Wang et al. prepared graphitic porous carbon nanosheets (GPCSs) from straw waste via an integrated Zn salt activation and graphitization treatment. Benefiting from the graphitic carbon sheets and abundant pores in the carbon framework, the GPCSs showed a large specific surface area and good wettability and conductivity, contributing to a good deionization capacity of 19.3 mg/g at 1.2 V in 500 mg/L NaCl solution [208]. Aside from Zn salt activation, KOH modification [207,209,210], calcination temperature control [211], and microwave treatment [212,213] are also powerful methods to enlarge the specific surface area and regulate the porosity of carbon materials.

Introducing dopants and functional groups can enhance carbon materials' electrochemical deionization performance [214–216]. Chang et al. found that the N and S co-doped carbon (NS-C) from plastic wastes held higher deionization capacities and faster deionization rates than those of the single-element (N or S) doped carbon. The improved performance of NS-C in the removal of heavy metal ions could be attributed to the large accessible specific surface area and the deeply AC surface by rich heteroatom doping sites (~4.55 at% N and ~13.30 at% S) [217]. A recent study suggested that the N, S, O-co-doped porous carbon (NSO-PC) obtained from buckwheat husk exhibited a high electrosorption capacity (12.7 mg/g in 500 mg/L NaCl solution at 1.2 V), a high charge efficiency (over 0.9), and good reusability (the electrosorption capacity retained 96% after 30 cycles) in the capacitive deionization (CDI) application [214]. The N, S, and O dopants improved the deionization performance via enlarging the specific surface area, regulating the porous structure, enhancing the wettability, providing faradaic pseudocapacitance, and facilitating the adsorption and distribution of ionic charges. Adding functional groups to biochar can enhance pollutant removal capacity and ion selectivity. Stephanie et al. found that the sulfonate and amine groups

functionalized biochar showed an enhanced electrosorption capacity and improved charge efficiency than the bare biochar because the ion-selective functional groups ameliorated the wettability and provided more ion transport inside the pore of the electrode [218]. Wang and coworkers found that the quaternary ammonium nitrogen functionalized mesoporous biochar presented a high electrosorption capacity of 28.31 mg/g toward 20 mg/L ClO_4^- at 1 V. The good electrosorption activity should contribute to the increased specific surface area and regulated pore structure via ZnO activation, as well as the improved surface wettability and conductivity caused by quaternary amine nitrogen (Figure S3a) [219].

Compositing biochar with electroactive components for electrochemical deionization has gained growing interest. For example, the Ag nanospheres incorporated biomass waste-derived AC (Ag/P-AC) was synthesized via a multi-step process and employed in the electrosorption of NaCl and toxic metal ions within a CDI system (Figure S3b) [206]. Using Ag/P-AC as the anode and P-AC as the cathode, the asymmetric Ag/P-AC//P-AC based CDI system possessed a higher NaCl electrosorption capacity over the P-AC//P-AC-based symmetric system (36 vs. 22.7 mg/g). Additionally, the asymmetric CDI system was more suitable for anions adsorption than the symmetric one. Metal oxides/biochar composites also retain good capacities for electrochemical deionization application because the pseudocapacitive property of metal oxides derived from reversible and fast Faradaic reactions can synergistically improve the electrochemical performance when combined with biochar [220–223]. Rambabu et al. synthesized a watermelon-derived AC (WMAC)/$MnFe_2O_4$ composite (WMAC/$MnFe_2O_4$) via a pyrolysis-hydrothermal process (Figure S3c). Based on the principle of the analogous desalination battery system, the WMAC/$MnFe_2O_4$ electrode attained a high NaCl electrosorption capacity of 29.7 mg/g, with rapid desalination and good recyclability (Figure S3d) [224].

Apart from biomass and plastic wastes, industrial and electronic wastes have also been used in the electrochemical deionization application [225–227]. For instance, Weng and coauthors developed activated microporous carbon spheres (AMCS) from anode materials of spent Li-ion batteries, which could be employed as efficient CDI electrodes. With a high specific surface area (2626 m^2/g) and pore volume of (0.98 cm^3/g), the AMCS demonstrated good NaCl electrosorption capacity (12.73 mg/g) and a fast salt adsorption rate (2.64 mg/(g·min)) at 1.2 V [227].

5.2. Waste-derived materials for pollutant electrodegradation

As a destructive technology for pollutant degradation, electrocatalysis has made great progress in wastewater treatment because of its high effectiveness, high energy efficiency, and easy implementation [4,34]. It is widely recognized that electrocatalysts/electrodes play a central role in pollutant degradation, and designing cheap and efficient catalysts is an important task. In this context, waste (e.g., biomass wastes, sludge, industrial wastes)-derived materials have been extensively implemented for contaminant electrodegradation [228,229]. With good electrical conductivity, large specific surface area, high chemical resistance, and flexible, functional groups, biochar is widely applied as the electrocatalyst or the support for metal-based electroactive materials. Liu and coauthors found that Fe and Zn-modification enlarged the specific surface area and surface functional groups of biochar and enhanced the adsorption and electrolysis of nitrobenzene [230]. Since the electrocatalytic performance of catalysts highly depends on their nanostructure and electronic properties [191,193,231–233], more studies loaded electroactive materials on porous biochar and formed composites for electrocatalytic applications [234–236]. Starting from municipal sludge, Zhao and coworkers developed a Pd/sludge-biochar loaded foam nickel electrode (Pd-SAC@Ni) for the electroreductive degradation of 4-chlorophenol (4-CP) (Figure S4a) [237]. Under a current density of 5 mA/cm^2, the removal efficiency of 4-CP reached 98.9% within 2 h, with an initial concentration of 0.8 mM. The indirect and direct reduction pathways were both involved in the 4-CP electrodegradation process, and their contributions were 80.5% and 19.5%, respectively. In a similar Pd/N-doped loofah sponge-derived biochar electrode, the N dopant played an important role in the electroreduction of bromate by enhancing the adsorption ability and electrocatalytic activity of the composite electrode [238]. Aside from these noble metals, transition metal-based oxides and sulfides are also employed to construct composite with biochar. Zhou et al. found that the porous structure of TiO_2/tea porous carbon (TPC) composite created a large number of good channels for electron transport and promoted the yield of hydroxyl radicals (·OH) in the degradation of phenol [47]. Gong and coworkers designed an O and N-enriched hierarchical MoS_2 nanospheres decorated with cornstalk-derived AC (MoS_2/CSAC) for phenol degradation. The hierarchical structure of the MoS_2/CSAC composite contributed to more catalytic active sites, and the abundant mesopores with diverse pore sizes benefited fast electrocatalytic reactions. In addition, the coexistence of Mo^{6+} and Mo^{4+} species in the MoS_2/CSAC composite accelerated the formation of ·OH from H_2O_2 (Figure S4b) [236].

The development of three-dimensional electrochemical reactors (3DERs) is a breakthrough in electrochemical pollutant degradation due to the high mass transfer, high current efficiency, easy operation, and high area-to-volume ratio [239,240]. In a 3DER, the particle electrode governs the electrocatalytic efficiency. A Ti-Sn-Ce/bamboo biochar (BC) composite was synthesized and used as particle electrodes in a 3DER for coking wastewater treatment (Figure S4c-d). The BC possessed compact and uniform pores, and the metal oxides effectively covered the internal pore surface of the biochar support. These structure and chemical compositional features contributed to an enhanced degradation performance of the BC particle electrode [239]. Apart from these biochar-based composites, industrial flotation tailings have also been adopted as particle electrodes for the degradation of TC in a three-dimensional aeration electrocatalysis reactor (3D-AER) (Figure S4e). The flotation tailings particle electrode (FPE) exhibited a high TC adsorption capacity, and the adsorption-saturated FPE could be regenerated by an electrochemical process to induce further absorption and form *in situ* electrodegradation [34].

6. Waste-derived materials for AOPs

AOPs utilizing powerful hydroxyl (·OH) or sulfate radicals ($SO_4^{\cdot-}$) as the major oxidizing active species have gained growing attention in wastewater treatment due to their great potential in removing anthropogenic pollutants [241]. Generally, nanomaterials are involved in the activation of oxidizers and the subsequent oxidation process, and waste-derived materials (especially carbon materials) are extensively studied, as depicted in Table S3.

6.1. Waste-derived materials for hydroxyl radical-based AOPs

Hydroxyl radicals (·OH) are a kind of powerful and nonselective oxidizing agent, with an oxidation potential of 2.8 V vs. NHE (normal hydrogen electrode, pH = 0) and a short lifetime ($t_{1/2} \leq 1$ μs). Hydroxyl radicals can attack organic pollutants through four basic mechanisms: radical addition, radical combination, hydrogen abstraction, and electron transfer [242,243]. Since hydroxyl radicals show a very short lifetime, they are generally *in situ* generated during application by various methods, including a combination of oxidizing agents (e.g., H_2O_2), catalysts (e.g., Fe^{2+}, carbon), and/or irradiation (e.g., ultraviolet light) [244]. In this context, controlling the production of hydroxyl radicals via using waste-derived catalysts would benefit the water treatment process.

Waste-derived metal-bearing Fenton-like catalysts (such as those containing Fe, Cu, Cr, Co, Ce, and Ru) are widely used due to their high efficiency in the decomposition of H_2O_2 to ·OH [245–247]. For instance, Wang et al. developed iron-doped biochar (Fe@BC) Fenton-like catalyst

from sawdust, which presented high degradation performance toward RhB (over 92.7% degradation within 140 min). In addition, the biochar support of Fe@BC was ineffective in activating H_2O_2 for RhB removal, and iron species on biochar were central active sites for RhB degradation [248]. Similarly, diverse Fe-based Fenton catalysts have been designed from wastes (e.g., waste lithium-ion batteries [75], iron ore tailings [249], sludge [250,251], and biomass [252]) for organic contaminant degradation. Aside from Fe-based catalysts, Cu-based Fenton-like catalysts synthesized from WPCBs also held a good performance for RhB degradation (a removal efficiency of 95.78% within 6 h at neutral pH) [253]. Given the differences in the electronic properties of various metals, constructing dual/triple metal active sites would enhance the production of hydroxyl radicals. It should be noted that the difference in pollutants' concentration between actual water (μg/L level) and simulated sewage (mg/L level) severely hinders the application of Fenton-like oxidation in natural wastewaters. To overcome this challenge, Zhou et al. designed an adsorptive catalyst from waste leather to degrade trace SMX. First, the adsorptive catalyst (WLBC) was able to effectively adsorb trace SMX via hydrophobic interaction, electrostatic attraction, π-π interaction, etc. Then, the oxidation of SMX by the *in situ* produced ·OH from WLBC mediated Fenton-like process could recover WLBC's adsorption ability (Figure S5a) [254]. The integrated adsorption and *in situ* Fenton-like oxidation process enables the removal of organic pollutants with low concentrations.

Metal leakage is a general problem of metal-bearing Fenton-like catalysts, which leads to performance degradation and metallic sludges [255]. Hence, metal-free Fenton-like catalysts from biowaste have attracted great interest. For example, Zhuang and co-workers developed a metal-free 3D graphene-based Fenton-like catalyst (OG) from biowastes [245]. Compared with the common two-dimensional (2D) graphene structure, the 3D graphene assembly associated with the confinement effect of OG led to a smaller energy barrier (1.1 vs. 1.6 eV) for the decomposition of H_2O_2. In addition, the electron migration via the C–O–C bridge in OG increased electron loss from the C–F bonds and facilitated the mineralization of perfluorooctanoic acid (PFOA). These structural and electronic properties of OG contributed to a high degradation performance (93.4% of PFOA was removed in 150 min).

Waste-derived catalysts involving field-assisted Fenton-like processes can degrade pollutants effectively. Sono-Fenton-like, photo-Fenton-like, and electro-Fenton-like catalytic oxidation has attracted great interest. Sonolysis is capable of producing ·OH and other strong ROS through the thermal dissociation of water vapor inside the cavitation bubble during the transient collapse and improving the mass transfer efficiency in the reaction medium via intensive microturbulence and micromixing [256,257]. Coupling sonolysis with a Fenton-like process is thus of great efficiency for organic degradation [258,259]. Chu et al. studied the applicability of waste antivirus copper film (CF) as a Fenton-like catalyst in the sono-Fenton-like catalytic oxidation of BPA (Figure S5b) [256]. The degradation of BPA was significantly enhanced by ultrasound irradiation, and both surface-bound and free ·OH participated in the pollutant degradation under the sono-Fenton-like process using CF as the catalyst.

The Fenton-like process can also be intensified by the application of solar radiation, namely the photo-Fenton-like process [260]. Thus, the optical properties of catalysts are important for degradation performance. Nasuha and coworkers found that the magnetic-activated electric arc furnace slag (A-EAFS) was an effective Fenton-like catalyst for the photodegradation of MB and acid blue 29 (AB29) [261]. The A-EAFS provided additional Fe_3O_4 due to the changes in the iron oxide phase and its favorable response to visible light. Taking advantage of metal oxides' good photoactivity, spent Li-ion batteries [262] and sludge [263] have been employed to design photo-Fenton-like catalysts for organic degradation. Photoactive sulfides also attract scientific interest. Chen et al. developed CuS nanoparticles embedded with carbon nanosheets (CuS@CNs) using waste biomass-derived hydrogel as a template, which performed well for degrading 2,4-dichlorophenol in a photo-Fenton-like system [264]. The introduction of CNs significantly improved the separation of photogenerated charge carriers to stimulate the degradation of pollutants by CuS.

Compared with sono-Fenton-like and photo-Fenton-like oxidation, electro-Fenton systems gain more attention due to the advantage of *in situ* H_2O_2 generation through electrochemical oxygen reduction reaction (ORR). Both the selective generation of H_2O_2 and the conversion of H_2O_2 to ·OH significantly depend on the cathode catalysts [265,266]. Significant progress has been made in applying waste-derived materials as high-performance cathode catalysts in the electro-Fenton process. Figure S6 shows a general electro-Fenton system in which the nickel foam cathode was functionalized with a giant reed-derived N-doped biochar [267]. The obtained B@Ni-F cathode demonstrated a high ORR activity and H_2O_2 selectivity (70.41%) due to the rich pyridinic N and O-bearing groups on the biochar. Along with the Fe-F catalyst, the B@Ni-F involved electro-Fenton system enabled the efficient degradation of sulfamerazine (SMR). This study also emphasized the importance of electrolytes. Using polyphosphate-based electrolytes induced enhanced SMR degradation. This should be linked with the improved generation of ·OH from Fe^{2+}-polyphosphate ligand complexes through the activation of O_2. To reduce the energy consumption of the electro-Fenton process, the self-powered electro-Fenton degradation system based on triboelectric nanogenerator (TENG) technology realizes pollution mineralization in an eco-friendly and energy-saving manner [268]. Zhu et al. synthesized N-doped biomass carbon catalysts for a self-powered electro-Fenton system. This system combines 3D printed flexible multilayered TENG (PFM-TENG) with the N-doped porous carbon as the electro-Fenton catalyst (Fig. 4). With a high surface area (1790.8 m^2/g) and a high content of N/O dopants (20.6 at%), the waste-derived cathode-driven electro-Fenton process enabled high degradation efficiencies of crystal violet (95.4%) and orange IV (96.0%) in 1 h [269]. Furthermore, waste-derived cathodes can also realize an effective neutral Fe-free electro-Fenton process. As reported, the bamboo-derived graphitic biochar (GB) could support O_2 reduction and H_2O_2 activation at pH 7 simultaneously. The composite cathode that combined GB with stainless steel mesh (GBSS) was able to remove various model pollutants (4-nitrophenol, orange II, reactive blue 19) effectively within 2 h, in the absence of Fe salts [270]. Beyond electrochemistry-assisted Fenton reaction, the heterogeneous visible-light-driven photo-electro-Fenton (H-VL-PEF) system based on N/O biomass self-doped porous carbon (NO/PC) cathode demonstrated a high degradation performance toward tetracycline [271]. In the H-VL-PEF process, the introduction of $CuFeO_2$/biochar catalysts and visible light decreased energy consumption and improved pollutant mineralization efficiency via promoting $\equiv Cu^{2+}/\equiv Cu^{+}$ and $\equiv Fe^{3+}/\equiv Fe^{2+}$ redox cycles and benefiting $\cdot OH/O_2^{\cdot-}$ formation. These modified electro-Fenton systems promote the development of low-cost and efficient techniques for organic pollutant degradation based on hydroxyl radicals.

6.2. Waste-derived materials for sulfate radical-based AOPs

AOPs based on $SO_4^{\cdot-}$ gain significant attention due to the high redox potential (2.5–3.1 V vs. NHE), long half-life time ($t_{1/2}$ = 30–40 μs), and fast pollutant degradation rate (10^6–10^9/(M·s)) of $SO_4^{\cdot-}$ [50]. $SO_4^{\cdot-}$ can be produced from peroxydisulfate (PDS) or PMS activated by catalysts, ultrasound, heat, UV light, electro-chemistry method, etc [44,49]. Currently, a crucial issue is to develop low-cost and efficient catalysts to activate PDS/PMS, and waste-derived materials have presented their advantages such as high catalytic efficiency, low price, and environmental friendliness [48].

Metal-bearing industrial and electronic wastes can be converted to activators for PDS/PMS [272]. Rahimi et al. found that the grounded pyrite (FeS_2) mine waste could be directly employed as nontoxic catalysts for PMS activation to oxidize tetracycline [273]. Simultaneous generation of $SO_4^{\cdot-}$ and ·OH was observed in the pyrite/PMS system, and a high tetracycline (50 mg/L) degradation efficiency of 98.3% was attained

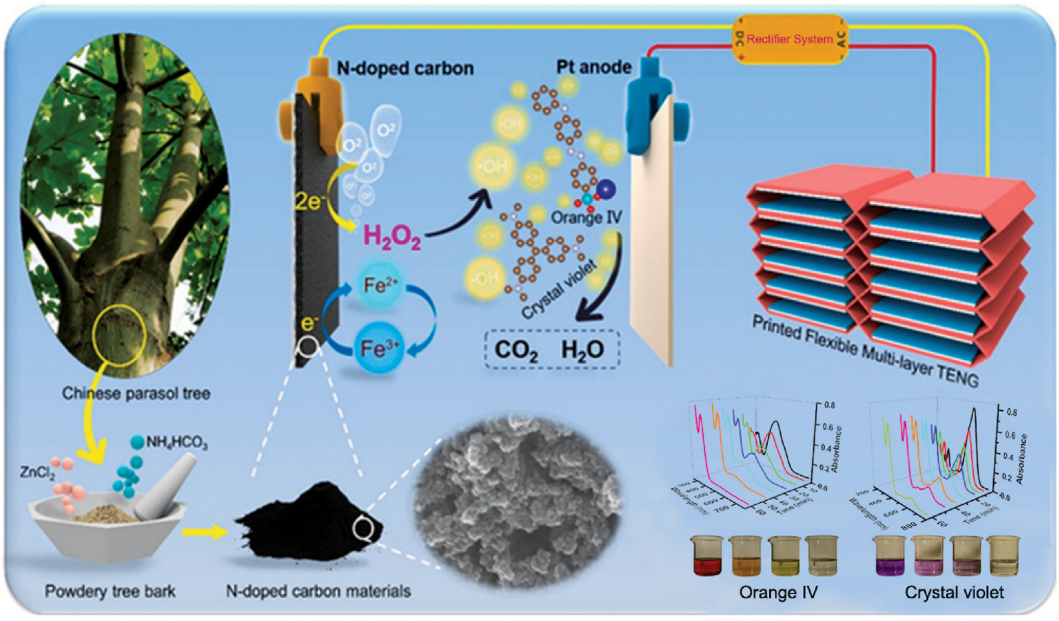

Fig. 4. Waste-derived materials for hydroxyl radical-based advanced oxidation processes. Schema of an energy-saving electro-Fenton system based on biochar and triboelectric nanogenerator (TENG) technology [269], Copyright © 2021, Elsevier.

within 30 min. Rahimi and coauthors developed a Fe-containing carbonaceous catalyst (PMCW) from coagulation wastes, which displayed a good performance in activating PMS for degradation of Reactive Red 2 (RR2). Both radical and nonradical pathways contributed to RR2 decomposition in the PMCW/PMS system. Apart from ROS ($SO_4^{\cdot-}$, ·OH, and $^1O_2$), the –OH and π-π* system-induced electron transfer also contributed to the reaction [274]. Starting from iron sludge, Zhu et al. designed a dual-active metal component on SiO_2 (Co-Fe/SiO_2 LC) as the activator of PMS for the mineralization of ciprofloxacin (CIP) (Fig. 5) [275]. A synergistic effect between Fe and Co was witnessed on the catalyst's surface because Fe^{2+} accelerated the reduction of Co^{3+}. In addition, both ·OH and $SO_4^{\cdot-}$ were produced in the PMS activation process, and $SO_4^{\cdot-}$ dominated the CIP degradation process. Similarly, a Fe/Mn-based catalyst (MS-N3H) derived from electrolytic manganese slag could activate PMS for levofloxacin degradation [276]. In the degradation of levofloxacin, both radical and nonradical pathways were disclosed. The rich Mn and Fe sites on the MS-N3H catalyst surface contributed to the formation of $SO_4^{\cdot-}$, ·OH, and $O_2^{\cdot-}$ radicals, and the lattice oxygen benefited the nonradical $^1O_2$ production. Thus, the successive oxidation reaction induced by active species led to the efficient decomposition of levofloxacin (degradation rate of 82.6% in 2 h). Besides these Fe-based wastes, copper oxide derived from the anode electrode of spent lithium-ion batteries was capable of activating PMS for degradation of various organic contaminants (e.g., RhB, MO) [277]. The redox cycle of Cu(II)/Cu(I) in the catalyst was the main force to drive PMS activation for the generation of active oxygen species, in which $SO_4^{\cdot-}$ and $^1O_2$ exerted a dominant effect.

Metal-free biochar also demonstrates good catalytic performance for PMS/PDS activation, and the surface functional groups and N dopants play a central role in enhancing pollutants' degradation properties [278, 279]. Wang et al. developed an N-doped biochar catalyst from agricultural waste pomelo peel. The N-doped biochar exhibited a high specific

Fig. 5. Waste-derived materials for sulfate radical-based advanced oxidation processes. The preparation of Co–Fe/SiO_2 LC and the catalytic mechanisms of PMS [275], Copyright © 2020, Elsevier.

surface area (738 m^2/g) and a high level of nitrogen content (13.54 at%) [280]. Integrating with rich defects, carbonyl groups, and high content of pyrrolic N and graphitic N, the N-doped biochar showed high catalytic performance for PMS activation to degrade SMX (95% of the pollutant was removed within 30 min) via a nonradical oxidation process. Similarly, in a passion fruit shell-derived biochar (PFSC)/PMS system for tetracycline hydrochloride degradation, the graphitic N atoms and the carboxyl group of ketones were the possible active sites of the nonfree radical pathway, including the formation of $O_2^{\cdot-}$/$^1O_2$ or direct electron transfer [281]. To this end, the catalytic performance of biochar can be improved via chemical component regulation, which can be achieved by selecting suitable biomass precursors and optimizing the pyrolysis parameters.

To enhance the catalytic performance of biochar, developing transition metal-bearing/doping biochar and constructing metal component/biochar composites are extensively studied. By using waste watermelon peel as the starting material, a co-doped carbon aerogel catalyst (Co–CA) was synthesized by a hydrothermal method. The Co–CA catalyst was capable of activating PMS for 2, 4-dichlorophenol (2, 4-DCP), CIP, and BPA degradation in various water matrices. The PMS activation mainly followed two pathways, radical (·OH and $SO_4^{\cdot-}$) pathways and nonradical ($^1O_2$) pathways, depending on the Co^{2+}/Co^{3+} redox cycle [282]. In a sludge-derived biochar/PS system, the Fe^{2+}/Fe^{3+} redox cycle also influenced the generation of active $SO_4^{\cdot-}$ and $O_2^{\cdot-}$ for the degradation of 4-chlorophenol [283]. Combining biochar with metal-based materials enables improved catalytic performance. For a biochar-supported iron sulfide (Fe_xS_y) composite (Fe_xS_y@biochar), the high catalytic performance of Fe_xS_y@biochar for PS activation was mainly attributed to the production of free radicals (·OH and $SO_4^{\cdot-}$) induced by Fe_xS_y particles on biochar, followed by the possible activation by oxygen-containing functional groups [284]. Benefiting from the advantages of metals' redox properties and carbon's high conductivity and large surface area, ZVI-sludge derived biochar/PS system [285], Ag_2O-Ag-waste eggshell/PMS system [286], and FeClO-sludge derived biochar/PMS system [287] also possess high performance for organic degradation.

7. Conclusions and perspectives

Developing waste-derived functional materials for wastewater remediation is significant in ensuring sustainable clean water security. Herein, the recent applications of waste (e.g., biomass wastes, electronic wastes, and industrial wastes)-derived materials for wastewater purification are reviewed. Sophisticated strategies like pyrolysis and combustion, hydrothermal synthesis, sol–gel method, coprecipitation, and ball milling for turning wastes into functional materials are first analyzed. Also, critical experimental parameters within different design strategies are discussed. After that, recent applications of waste-derived functional materials in adsorption, photocatalytic degradation, electrochemical treatment, and AOPs are detailed. The advancement of efficient functional materials via regulating the internal and external characteristics of waste-derived materials is well illustrated, and the material's property–performance correlation is emphasized.

Currently, although great progress has been achieved in the development of waste-derived materials for wastewater remediation, there remain some critical issues that deserve further investigation. First, exploring more waste precursors for the design of cost-effective materials for wastewater purification is needed. Currently, biomass wastes have been well explored, while industrial and electronic wastes attract less attention. Because of the negative environmental impacts and favorable metal-rich features, the conversion of industrial and electronic wastes into functional materials may have high environmental and economic values. Second, for the application of waste-derived materials, the purity of materials should be well examined since the chemical composition profoundly affects their performance. Third, integrating advanced characterization techniques (e.g., Raman spectroscopy, microscopy, spectroscopy, and X-ray absorption spectroscopy) with computational tools can facilitate the understanding of the materials' structure–performance correlation and optimize the material design/synthesis. Furthermore, novel strategies are required to design materials with low fabrication costs and high performance, and strategies with a short process and low-carbon emissions are highly favorable for achieving the carbon neutrality goal. In addition, since many waste-derived materials work in different techniques, the applications of waste-derived materials in integrated technologies (e.g., adsorption-AOP process, electro-Fenton process, photo-Fenton process, photo-assisted PMS activation process, and bio-electrochemical system) for wastewater remediation may upgrade the performance and decrease the operational costs. In addition, coupling solar energy with the wastewater treatment process (e.g., electrochemical degradation) can reduce the utilization of fossil fuels and further limit carbon emissions. Last, it is of great significance to apply waste-derived functional materials in other rising fields, such as electrochemical water splitting, by which we can develop a carbon-free energy system.

Declaration of competing interests

The authors have declared no conflict of interest.

Acknowledgments

This work is supported by the Australian Research Council Discovery Project (DP220101139). Zhijie Chen thanks the support of the Post Thesis Award from the University of Technology Sydney. Dr. Wei acknowledges the support of the Australian Research Council through project DE220100530.

Appendix A. Supplementary data

Supplementary data to this article can be found online at https://doi.org/10.1016/j.eehl.2022.05.001.

References

[1] D.B. Miklos, C. Remy, M. Jekel, K.G. Linden, J.E. Drewes, U. Hübner, Evaluation of advanced oxidation processes for water and wastewater treatment–A critical review, Water Res 139 (2018) 118–131, https://doi.org/10.1016/j.watres.2018.03.042.
[2] K. Paździor, L. Bilińska, S. Ledakowicz, A review of the existing and emerging technologies in the combination of AOPs and biological processes in industrial textile wastewater treatment, Chem Eng J 376 (2019), 120597, https://doi.org/10.1016/j.cej.2018.12.057.
[3] Q.-S. Huang, W. Wu, W. Wei, L. Song, J. Sun, B.-J. Ni, Highly-efficient Pb^{2+} removal from water by novel $K_2W_4O_{13}$ nanowires: performance, mechanisms and DFT calculation, Chem Eng J 381 (2020), 122632, https://doi.org/10.1016/j.cej.2019.122632.
[4] Z. Chen, Y. Liu, W. Wei, B.-J. Ni, Recent advances in electrocatalysts for halogenated organic pollutant degradation, Environ Sci: Nano 6 (2019) 2332–2366, https://doi.org/10.1039/C9EN00411D.
[5] R. Zheng, J. Li, R. Zhu, R. Wang, X. Feng, Z. Chen, et al., Enhanced Cr(VI) reduction on natural chalcopyrite mineral modulated by degradation intermediates of RhB, J Hazard Mater 423 (2021), 127206, https://doi.org/10.1016/j.jhazmat.2021.127206.
[6] N. Li, M. He, X. Lu, B. Yan, X. Duan, G. Chen, et al., Municipal solid waste derived biochars for wastewater treatment: production, properties and applications, Resour, Conserv Recycl 177 (2022), 106003, https://doi.org/10.1016/j.resconrec.2021.106003.
[7] Q. Hao, G. Jia, W. Wei, A. Vinu, Y. Wang, H. Arandiyan, et al., Graphitic carbon nitride with different dimensionalities for energy and environmental applications, Nano Res 13 (2019) 18–37, https://doi.org/10.1007/s12274-019-2589-z.
[8] Z. Chen, W. Wei, H. Chen, B.-J. Ni, Eco-designed electrocatalysts for water splitting: a path toward carbon neutrality, Int J Hydrogen Energy (2022), https://doi.org/10.1016/j.ijhydene.2022.03.046.
[9] H. Chen, Z. Chen, W. Wei, W. Zou, J. Li, R. Zheng, et al., Integrating electrodeposition with electrolysis for closing loop resource utilization of battery industrial wastewater, Green Chem (2022), https://doi.org/10.1039/D1GC04891K.
[10] S.O. Amusat, T.G. Kebede, S. Dube, M.M. Nindi, Ball-milling synthesis of biochar and biochar–based nanocomposites and prospects for removal of emerging contaminants: a review, J Water Process Eng 41 (2021), 101993, https://doi.org/10.1016/j.jwpe.2021.101993.

[11] S.M. Abdelbasir, K.M. McCourt, C.M. Lee, D.C. Vanegas, Waste-derived nanoparticles: synthesis approaches, environmental applications, and sustainability considerations, Front Chem 8 (2020) 782, https://doi.org/10.3389/fchem.2020.00782.
[12] R. Shan, J. Han, J. Gu, H. Yuan, B. Luo, Y. Chen, A review of recent developments in catalytic applications of biochar-based materials, Resour, Conserv Recycl 162 (2020), 105036, https://doi.org/10.1016/j.resconrec.2020.105036.
[13] A. Batool, S. Valiyaveettil, Chemical transformation of soya waste into stable adsorbent for enhanced removal of methylene blue and neutral red from water, J Environ Chem Eng 9 (2021), 104902, https://doi.org/10.1016/j.jece.2020.104902.
[14] N. Liu, Y. Liu, G. Zeng, J. Gong, X. Tan, S. Liu, et al., Adsorption of 17β-estradiol from aqueous solution by raw and direct/pre/post-KOH treated lotus seedpod biochar, J Environ Sci 87 (2020) 10–23, https://doi.org/10.1016/j.jes.2019.05.026.
[15] H. Çelebi, Recovery of detox tea wastes: usage as a lignocellulosic adsorbent in Cr^{6+} adsorption, J Environ Chem Eng 8 (2020), 104310, https://doi.org/10.1016/j.jece.2020.104310.
[16] R.J. Ramalingam, M. Sivachidambaram, J.J. Vijaya, H.A. Al-Lohedan, M. Muthumareeswaran, Synthesis of porous activated carbon powder formation from fruit peel and cow dung waste for modified electrode fabrication and application, Biomass Bioenergy 142 (2020), 105800, https://doi.org/10.1016/j.biombioe.2020.105800.
[17] J. Wu, X. Yan, L. Li, J. Gu, T. Zhang, L. Tian, et al., High-efficiency adsorption of Cr (VI) and RhB by hierarchical porous carbon prepared from coal gangue, Chemosphere 275 (2021), 130008, https://doi.org/10.1016/j.chemosphere.2021.130008.
[18] W. Wu, Z. Chen, Y. Huang, J. Li, D. Chen, N. Chen, et al., Red mud for the efficient adsorption of U (VI) from aqueous solution: influence of calcination on performance and mechanism, J Hazard Mater 409 (2021), 124925, https://doi.org/10.1016/j.jhazmat.2020.124925.
[19] M. Jiang, Y. Yang, T. Lei, Z. Ye, S. Huang, X. Fu, et al., Removal of phosphate by a novel activated sewage sludge biochar: equilibrium, kinetic and mechanism studies, Appl Energy Combust Sci (2022), 100056, https://doi.org/10.1016/j.jaecs.2022.100056.
[20] U.A. Edet, A.O. Ifelebuegu, Kinetics, isotherms, and thermodynamic modeling of the adsorption of phosphates from model wastewater using recycled brick waste, Processes 8 (2020) 665. https://www.mdpi.com/2227-9717/8/6/665.
[21] P. Hadi, J. Barford, G. McKay, Toxic heavy metal capture using a novel electronic waste-based material-mechanism, modeling and comparison, Environ Sci Technol 47 (2013) 8248–8255, https://doi.org/10.1021/es4001664.
[22] W. Zou, X. Feng, W. Wei, Y. Zhou, R. Wang, R. Zheng, et al., Converting spent $LiFePO_4$ battery into zeolitic phosphate for highly efficient heavy metal adsorption, Inorg Chem 60 (2021) 9496–9503, https://doi.org/10.1021/acs.inorgchem.1c00614.
[23] C.-K. Tsai, R.-a. Doong, H.-Y. Hung, Sustainable valorization of mesoporous aluminosilicate composite from display panel glasses waste for adsorption of heavy metal ions, Sci Total Environ 673 (2019) 337–346, https://doi.org/10.1016/j.scitotenv.2019.04.056.
[24] T.-H. Liou, S.-M. Liu, G.-W. Chen, Utilization of e-wastes as a sustainable silica source in synthesis of ordered mesostructured titania nanocomposites with high adsorption and photoactivity, J Environ Chem Eng 10 (2022), 107283, https://doi.org/10.1016/j.jece.2022.107283.
[25] B. Greene, M. Hosea, R. McPherson, M. Henzl, M.D. Alexander, D.W. Darnall, Interaction of gold (I) and gold (III) complexes with algal biomass, Environ Sci Technol 20 (1986) 627–632, https://doi.org/10.1021/es00148a014.
[26] J. Pradhan, J. Das, S. Das, R.S. Thakur, Adsorption of phosphate from aqueous solution using activated red mud, J Colloid Interface Sci 204 (1998) 169–172, https://doi.org/10.1006/jcis.1998.5594.
[27] G. Salitra, A. Soffer, L. Eliad, Y. Cohen, D. Aurbach, Carbon electrodes for double-layer capacitors I. Relations between ion and pore dimensions, J Electrochem Soc 147 (2000) 2486, https://doi.org/10.1149/1.1393557.
[28] F.-S. Zhang, J.O. Nriagu, H. Itoh, Photocatalytic removal and recovery of mercury from water using TiO_2-modified sewage sludge carbon, J Photochem Photobiol, A 167 (2004) 223–228, https://doi.org/10.1016/j.jphotochem.2004.06.001.
[29] B. Chen, D. Zhou, L. Zhu, Transitional adsorption and partition of nonpolar and polar aromatic contaminants by biochars of pine needles with different pyrolytic temperatures, Environ Sci Technol 42 (2008) 5137–5143, https://doi.org/10.1021/es8002684.
[30] T. Tsai, C. Kao, A. Hong, Treatment of tetrachloroethylene-contaminated groundwater by surfactant-enhanced persulfate/BOF slag oxidation-A laboratory feasibility study, J Hazard Mater 171 (2009) 571–576, https://doi.org/10.1016/j.jhazmat.2009.06.036.
[31] K. Natrchalayuth, T. Wasanapiarnpong, S. Larpkiattaworn, P. Sujaridworakun, Hydrothermal synthesis of zinc oxide nanoparticle from zinc-dust waste for photocatalytic and antibacterial applications, Adv Mater Res (2012) 78–81, https://doi.org/10.4028/www.scientific.net/AMR.506.78.
[32] C.-Y. Kuo, C.-Y. Pai, Application of cuprous oxide synthesized from copper-containing waste liquid to treat aqueous reactive dye, Water Sci Technol 65 (2012) 1557–1563, https://doi.org/10.2166/wst.2012.047.
[33] M. Baldissera, M. Silva, C. Silveira, R. Lima, S. Maia, M. da Silva, et al., Synthesis and characterization of Zn and Mn ferrites from spent batteries, Cerâmica 60 (2014) 52–56, https://doi.org/10.1590/S0366-69132014000100007.
[34] S. Yang, Y. Feng, D. Gao, X. Wang, N. Suo, Y. Yu, et al., Electrocatalysis degradation of tetracycline in a three-dimensional aeration electrocatalysis reactor (3D-AER) with a flotation-tailings particle electrode (FPE): physicochemical properties, influencing factors and the degradation mechanism, J Hazard Mater 407 (2021), 124361, https://doi.org/10.1016/j.jhazmat.2020.124361.
[35] X. Li, K. Hu, Y. Huang, Q. Gu, Y. Chen, B. Yang, et al., Upcycling biomass waste into Fe single atom catalysts for pollutant control, J Energy Chem 69 (2022) 282–291, https://doi.org/10.1016/j.jechem.2022.01.044.
[36] L. Liu, Y. Huang, S. Zhang, Y. Gong, Y. Su, J. Cao, et al., Adsorption characteristics and mechanism of Pb(II) by agricultural waste-derived biochars produced from a pilot-scale pyrolysis system, Waste Manag 100 (2019) 287–295, https://doi.org/10.1016/j.wasman.2019.08.021.
[37] S. Wang, W. Yan, F. Zhao, Recovery of solid waste as functional heterogeneous catalysts for organic pollutant removal and biodiesel production, Chem Eng J 401 (2020), 126104, https://doi.org/10.1016/j.cej.2020.126104.
[38] Z. Chen, R. Zheng, W. Zou, W. Wei, J. Li, W. Wei, et al., Integrating high-efficiency oxygen evolution catalysts featuring accelerated surface reconstruction from waste printed circuit boards via a boriding recycling strategy, Appl Catal B 298 (2021), 120583, https://doi.org/10.1016/j.apcatb.2021.120583.
[39] Z. Chen, W. Zou, R. Zheng, W. Wei, W. Wei, B.-J. Ni, et al., Synergistic recycling and conversion of spent Li-ion battery leachate into highly efficient oxygen evolution catalysts, Green Chem 23 (2021) 6538–6547, https://doi.org/10.1039/D1GC01578H.
[40] M. Graś, Ł. Kolanowski, Z. Chen, K. Lota, K. Jurak, J. Ryl, et al., Partial inhibition of borohydride hydrolysis using porous activated carbon as an effective method to improve the electrocatalytic activity of the DBFC anode, Sustainable Energy Fuels 5 (2021) 4401–4413, https://doi.org/10.1039/D1SE00999K.
[41] X. Li, X. Li, Y. Feng, X. Wang, N. Suo, S. Yang, et al., Production of an electro-biological particle electrode (EBPE) from lithium slag and its removal performance to salicylic acid in a three-dimensional electrocatalytic biological coupling reactor (3D-EBCR), Chemosphere 282 (2021), 131020, https://doi.org/10.1016/j.chemosphere.2021.131020.
[42] J. Cheng, T. Lu, S. Huang, G. Li, J. Wang, F. Kong, et al., Recovery of cobalt from spent lithium-ion batteries as the dopant of TiO_2 photocatalysts for boosting ciprofloxacin degradation, J Clean Prod 316 (2021), 128279, https://doi.org/10.1016/j.jclepro.2021.128279.
[43] A. Mahmoud, R.A. Hamza, E. Elbeshbishy, Enhancement of denitrification efficiency using municipal and industrial waste fermentation liquids as external carbon sources, Sci Total Environ (2021), 151578, https://doi.org/10.1016/j.scitotenv.2021.151578.
[44] C. Zhao, B. Shao, M. Yan, Z. Liu, Q. Liang, Q. He, et al., Activation of peroxymonosulfate by biochar-based catalysts and applications in the degradation of organic contaminants: a review, Chem Eng J 416 (2021), 128829, https://doi.org/10.1016/j.cej.2021.128829.
[45] S. Rangabhashiyam, P. Lins, L. Oliveira, P. Sepulveda, J.O. Ighalo, A.U. Rajapaksha, et al., Sewage sludge-derived biochar for the adsorptive removal of wastewater pollutants: a critical review, Environ Pollut 293 (2022), 118581, https://doi.org/10.1016/j.envpol.2021.118581.
[46] N.H. Solangi, J. Kumar, S.A. Mazari, S. Ahmed, N. Fatima, N.M. Mubarak, Development of fruit waste derived bio-adsorbents for wastewater treatment: a review, J Hazard Mater 416 (2021), 125848, https://doi.org/10.1016/j.jhazmat.2021.125848.
[47] P. Zhou, J. Wan, X. Wang, J. Chen, Y. Gong, K. Xu, et al., Preparation and electrochemical property of TiO_2/porous carbon composite cathode derived from waste tea leaves for electrocatalytic degradation of phenol, J Appl Electrochem 51 (2021) 653–667, https://doi.org/10.1007/s10800-020-01527-9.
[48] Z. Feng, R. Yuan, F. Wang, Z. Chen, B. Zhou, H. Chen, Preparation of magnetic biochar and its application in catalytic degradation of organic pollutants: a review, Sci Total Environ 765 (2021), 142673, https://doi.org/10.1016/j.scitotenv.2020.142673.
[49] P.V. Nidheesh, A. Gopinath, N. Ranjith, A. Praveen Akre, V. Sreedharan, M. Suresh Kumar, Potential role of biochar in advanced oxidation processes: a sustainable approach, Chem Eng J 405 (2021), 126582, https://doi.org/10.1016/j.cej.2020.126582.
[50] M.F. Gasim, J.W. Lim, S.C. Low, K.A. Lin, W.D. Oh, Can biochar and hydrochar be used as sustainable catalyst for persulfate activation? Chemosphere 287 (2022), 132458 https://doi.org/10.1016/j.chemosphere.2021.132458.
[51] I. Chakraborty, S.M. Sathe, B.K. Dubey, M.M. Ghangrekar, Waste-derived biochar: applications and future perspective in microbial fuel cells, Bioresour Technol 312 (2020), 123587, https://doi.org/10.1016/j.biortech.2020.123587.
[52] I. Anastopoulos, A. Bhatnagar, B.H. Hameed, Y.S. Ok, M. Omirou, A review on waste-derived adsorbents from sugar industry for pollutant removal in water and wastewater, J Mol Liq 240 (2017) 179–188, https://doi.org/10.1016/j.molliq.2017.05.063.
[53] T. Ahmad, M. Danish, Prospects of banana waste utilization in wastewater treatment: a review, J Environ Manage 206 (2018) 330–348, https://doi.org/10.1016/j.jenvman.2017.10.061.
[54] I.H. Alsohaimi, A.M. Nassar, T.A. Seaf Elnasr, B.A. Cheba, A novel composite silver nanoparticles loaded calcium oxide stemming from egg shell recycling: a potent photocatalytic and antibacterial activities, J Clean Prod 248 (2020) 119274, https://doi.org/10.1016/j.jclepro.2019.119274.
[55] R.H. Geraldo, A.R.D. Costa, J. Kanai, J.S. Silva, J.D. Souza, H.M. Andrade, et al., Calcination parameters on phosphogypsum waste recycling, Constr Build Mater 256 (2020), 119406, https://doi.org/10.1016/j.conbuildmat.2020.119406.
[56] M. Ahmad, A.U. Rajapaksha, J.E. Lim, M. Zhang, N. Bolan, D. Mohan, et al., Biochar as a sorbent for contaminant management in soil and water: a review, Chemosphere 99 (2014) 19–33, https://doi.org/10.1016/j.chemosphere.2013.10.071.

[57] X. Tan, S. Zhu, P.L. Show, H. Qi, S.-H. Ho, Sorption of ionized dyes on high-salinity microalgal residue derived biochar: electron acceptor-donor and metal-organic bridging mechanisms, J Hazard Mater 393 (2020), 122435, https://doi.org/10.1016/j.jhazmat.2020.122435.
[58] X. Hu, X. Zhang, H.H. Ngo, W. Guo, H. Wen, C. Li, et al., Comparison study on the ammonium adsorption of the biochars derived from different kinds of fruit peel, Sci Total Environ 707 (2020), 135544, https://doi.org/10.1016/j.scitotenv.2019.135544.
[59] J. He, Y. Xiao, J. Tang, H. Chen, H. Sun, Persulfate activation with sawdust biochar in aqueous solution by enhanced electron donor-transfer effect, Sci Total Environ 690 (2019) 768–777, https://doi.org/10.1016/j.scitotenv.2019.07.043.
[60] D. Bi, F. Huang, M. Jiang, Z. He, X. Lin, Effect of pyrolysis conditions on environmentally persistent free radicals (EPFRs) in biochar from co-pyrolysis of urea and cellulose, Sci Total Environ 805 (2022), 150339, https://doi.org/10.1016/j.scitotenv.2021.150339.
[61] E.S. Odinga, M.G. Waigi, F.O. Gudda, J. Wang, B. Yang, X. Hu, et al., Occurrence, formation, environmental fate and risks of environmentally persistent free radicals in biochars, Environ Int 134 (2020), 105172, https://doi.org/10.1016/j.envint.2019.105172.
[62] X. Ruan, Y. Sun, W. Du, Y. Tang, Q. Liu, Z. Zhang, et al., Formation, characteristics, and applications of environmentally persistent free radicals in biochars: a review, Bioresour technol 281 (2019) 457–468, https://doi.org/10.1016/j.biortech.2019.02.105.
[63] G.V. Sree, P. Nagaraaj, K. Kalanidhi, C. Aswathy, P. Rajasekaran, Calcium oxide a sustainable photocatalyst derived from eggshell for efficient photo-degradation of organic pollutants, J Clean Prod 270 (2020), 122294, https://doi.org/10.1016/j.jclepro.2020.122294.
[64] Y. Cheng, F. Luo, Y. Jiang, F. Li, C. Wei, The effect of calcination temperature on the structure and activity of TiO_2/SiO_2 composite catalysts derived from titanium sulfate and fly ash acid sludge, Colloids Surf, A 554 (2018) 81–85, https://doi.org/10.1016/j.colsurfa.2018.06.032.
[65] P. Tanniratt, T. Wasanapiarnpong, C. Mongkolkachit, P. Sujaridworakun, Utilization of industrial wastes for preparation of high performance ZnO/diatomite hybrid photocatalyst, Ceram Int 42 (2016) 17605–17609, https://doi.org/10.1016/j.ceramint.2016.08.074.
[66] A. Nath, A. Shah, L.R. Singh, M. Mahato, Waste plastic-derived NiO-MWCNT composite as visible light photocatalyst for degradation of methylene blue dye, Nanotechnol Environ Eng 6 (2021) 70, https://doi.org/10.1007/s41204-021-00163-8.
[67] M. Kumar Padhi, D. Rath, B.B. Nanda, P. Kar, B. Nanda, Solid waste derived montmorillonite clay as efficient photocatalytic system for removal of aquatic pollutants, Environ Nanotechnol Monit Manage 17 (2022), 100630, https://doi.org/10.1016/j.enmm.2021.100630.
[68] J. Xu, T. Zhang, J. Zhang, Photocatalytic degradation of methylene blue with spent FCC catalyst loaded with ferric oxide and titanium dioxide, Sci Rep 10 (2020), 12730, https://doi.org/10.1038/s41598-020-69643-2.
[69] H.S. Kambo, A. Dutta, A comparative review of biochar and hydrochar in terms of production, physico-chemical properties and applications, Renewable Sustainable Energy Rev 45 (2015) 359–378, https://doi.org/10.1016/j.rser.2015.01.050.
[70] J. Fang, L. Zhan, Y.S. Ok, B. Gao, Minireview of potential applications of hydrochar derived from hydrothermal carbonization of biomass, J Ind Eng Chem 57 (2018) 15–21, https://doi.org/10.1016/j.jiec.2017.08.026.
[71] X. Zhu, Y. Liu, F. Qian, C. Zhou, S. Zhang, J. Chen, Role of hydrochar properties on the porosity of hydrochar-based porous carbon for their sustainable application, ACS Sustainable Chem Eng 3 (2015) 833–840, https://doi.org/10.1021/acssuschemeng.5b00153.
[72] M.K. Sinha, S.K. Sahu, P. Meshram, L. Prasad, B.D. Pandey, Low temperature hydrothermal synthesis and characterization of iron oxide powders of diverse morphologies from spent pickle liquor, Powder Technol 276 (2015) 214–221, https://doi.org/10.1016/j.powtec.2015.02.006.
[73] L. Yu, D.N. Tran, P. Forward, M.F. Lambert, D. Losic, The hydrothermal processing of iron oxides from bacterial biofilm waste as new nanomaterials for broad applications, RSC Adv 8 (2018) 34848–34852, https://doi.org/10.1039/C8RA07061J.
[74] K. Liu, S. Liang, J. Wang, H. Hou, J. Yang, J. Hu, Synthesis of the PbS dendritic nanostructure recovered from a spent lead-acid battery via an integrated vacuum chlorinating and hydrothermal Process, ACS Sustainable Chem Eng 6 (2018) 17333–17339, https://doi.org/10.1021/acssuschemeng.8b04844.
[75] L. Xu, C. Chen, J.-B. Huo, X. Chen, J.-C.E. Yang, M.-L. Fu, Iron hydroxyphosphate composites derived from waste lithium-ion batteries for lead adsorption and Fenton-like catalytic degradation of methylene blue, Environ Technol Innovation 16 (2019), 100504, https://doi.org/10.1016/j.eti.2019.100504.
[76] J. Liang, Y. Xue, J.-n. Gu, J. Li, F. Shi, X. Guo, et al., Sustainably recycling spent lithium-ion batteries to prepare magnetically separable cobalt ferrite for catalytic degradation of bisphenol A via peroxymonosulfate activation, J Hazard Mater (2021), 127910, https://doi.org/10.1016/j.jhazmat.2021.127910.
[77] Z. Niu, X. Tao, H. Huang, X. Qin, C. Ren, Y. Wang, et al., Green synthesis of magnetically recyclable $Mn_{0.6}Zn_{0.4}Fe_2O_4$@$Zn_{1-x}Mn_xS$ composites from spent batteries for visible light photocatalytic degradation of phenol, Chemosphere 287 (2022), 132238, https://doi.org/10.1016/j.chemosphere.2021.132238.
[78] J. Tang, B. Mu, L. Zong, A. Wang, One-step synthesis of magnetic attapulgite/carbon supported NiFe-LDHs by hydrothermal process of spent bleaching earth for pollutants removal, J Clean Prod 172 (2018) 673–685, https://doi.org/10.1016/j.jclepro.2017.10.181.
[79] A. Durairaj, J. Liu, X. Lv, S. Vasanthkumar, T. Sakthivel, Facile synthesis of waste-derived carbon/MoS_2 composite for energy storage and water purification applications, Biomass Conv. Bioref, 2021, https://doi.org/10.1007/s13399-021-01396-y.
[80] A.A. Dolatabad, H. Ganjidoust, B. Ayati, Application of waste-derived activated red mud/base treated rice husk composite in sulfate adsorption from aqueous solution, Int J Environ Res 16 (2022) 1–16, https://doi.org/10.1007/s41742-021-00381-7.
[81] X. Jiang, P. Sun, L. Xu, Y. Xue, H. Zhang, W. Zhu, Platanus orientalis leaves based hierarchical porous carbon microspheres as high efficiency adsorbents for organic dyes removal, Chin J Chem Eng 28 (2020) 254–265, https://doi.org/10.1016/j.cjche.2019.03.030.
[82] J. Li, L. Xu, P. Sun, P. Zhai, X. Chen, H. Zhang, et al., Novel application of red mud: facile hydrothermal-thermal conversion synthesis of hierarchical porous AlOOH and Al_2O_3 microspheres as adsorbents for dye removal, Chem Eng J 321 (2017) 622–634, https://doi.org/10.1016/j.cej.2017.03.135.
[83] L. Cai, J. Sun, L. Cui, Y. Jiang, Z. Huang, Stabilization of heavy metals in piggery wastewater sludge through coagulation-hydrothermal reaction–pyrolysis process and sludge biochar for tylosin removal, J Cleaner Prod 260 (2020), 121165, https://doi.org/10.1016/j.jclepro.2020.121165.
[84] M. Parashar, V.K. Shukla, R. Singh, Metal oxides nanoparticles via sol–gel method: a review on synthesis, characterization and applications, J Mater Sci: Mater Electron 31 (2020) 3729–3749, https://doi.org/10.1007/s10854-020-02994-8.
[85] S. Obregón, V. Rodríguez-González, Photocatalytic TiO_2 thin films and coatings prepared by sol–gel processing: a brief review, J Sol-Gel Sci Technol (2021), https://doi.org/10.1007/s10971-021-05628-5.
[86] P. Huo, Y. Yan, S. Li, H. Li, W. Huang, Preparation of poly-o-phenylenediamine/TiO_2/fly-ash cenospheres and its photo-degradation property on antibiotics, Appl Surf Sci 256 (2010) 3380–3385, https://doi.org/10.1016/j.apsusc.2009.12.038.
[87] J. Qu, Y. Feng, Q. Zhang, Q. Cong, C. Luo, X. Yuan, A new insight of recycling of spent Zn–Mn alkaline batteries: synthesis of $Zn_XMn_{1-X}O$ nanoparticles and solar light driven photocatalytic degradation of bisphenol A using them, J Alloys Compd 622 (2015) 703–707, https://doi.org/10.1016/j.jallcom.2014.10.166.
[88] H. Nsubuga, C. Basheer, M.B. Haider, R. Bakdash, Sol-gel based biogenic silica composite as green nanosorbent for chemometric optimization of micro-solid-phase extraction of beta blockers, J Chromatogr A 1554 (2018) 16–27, https://doi.org/10.1016/j.chroma.2018.04.044.
[89] B. Deng, Y. Li, W. Tan, Z. Wang, Z. Yu, S. Xing, et al., Degradation of bisphenol A by electro-enhanced heterogeneous activation of peroxydisulfate using Mn-Zn ferrite from spent alkaline Zn-Mn batteries, Chemosphere 204 (2018) 178–185, https://doi.org/10.1016/j.chemosphere.2018.03.194.
[90] I.L. Santana, T.F.M. Moreira, M.F.F. Lelis, M.B.J.G. Freitas, Photocatalytic properties of Co_3O_4/$LiCoO_2$ recycled from spent lithium-ion batteries using citric acid as leaching agent, Mater Chem Phys 190 (2017) 38–44, https://doi.org/10.1016/j.matchemphys.2017.01.003.
[91] J.S. Ribeiro, T.F.M. Moreira, I.L. Santana, S.A.D. Ferreira, M.F.F. Lelis, M.B.J.G. Freitas, Sol-gel synthesis, characterization, and catalytic properties of Ni, Cd, Co, and Fe oxides recycled from spent Ni-Cd batteries using citric acid as a leaching agent, Mater Chem Phys 205 (2018) 186–194, https://doi.org/10.1016/j.matchemphys.2017.11.025.
[92] M.A. El-Kemary, I.M. El-mehasseb, K.R. Shoueir, S.E. El-Shafey, O.I. El-Shafey, H.A. Aljohani, et al., Sol-gel TiO_2 decorated on eggshell nanocrystal as engineered adsorbents for removal of acid dye, J Dispersion Sci Technol 39 (2018) 911–921, https://doi.org/10.1080/01932691.2017.1410829.
[93] L. Zhang, J. Guo, X. Huang, W. Wang, P. Sun, Y. Li, et al., Functionalized biochar-supported magnetic $MnFe_2O_4$ nanocomposite for the removal of Pb (II) and Cd (II), RSC Adv 9 (2019) 365–376, https://doi.org/10.1039/C8RA09061K.
[94] S. Li, J. Deng, L. Xiong, J. Wang, Y. Chen, Y. Jiao, et al., Design and construct CeO_2-ZrO_2-Al_2O_3 materials with controlled structures via co-precipitation method by using different precipitants, Ceram Int 44 (2018) 20929–20938, https://doi.org/10.1016/j.ceramint.2018.06.255.
[95] T.F.M. Moreira, I.L. Santana, M.N. Moura, S.A.D. Ferreira, M.F.F. Lelis, M.B.J.G. Freitas, Recycling of negative electrodes from spent Ni-Cd batteries as CdO with nanoparticle sizes and its application in remediation of azo dye, Mater Chem Phys 195 (2017) 19–27, https://doi.org/10.1016/j.matchemphys.2017.04.009.
[96] L.B. Magnago, A.K.S. Rocha, V.C.B. Pegoretti, S.A.D. Ferreira, M.F.F. Lelis, M.B.J.G. Freitas, $NiFe_2O_4$ synthesized from nickel recycled of spent Ni-MH batteries and their applications as a catalyst in a photo-Fenton process and as an electrochemical pseudocapacitor, Ionics 25 (2018) 2361–2372, https://doi.org/10.1007/s11581-018-2623-2.
[97] A.K. Singh, K. Ketan, J.K. Singh, Simple and green fabrication of recyclable magnetic highly hydrophobic sorbents derived from waste orange peels for removal of oil and organic solvents from water surface, J Environ Chem Eng 5 (2017) 5250–5259, https://doi.org/10.1016/j.jece.2017.09.060.
[98] N.I. Blaisi, M. Zubair, Ihsanullah, S. Ali, T.S. Kazeem, M.S. Manzar, et al., Date palm ash-MgAl-layered double hydroxide composite: sustainable adsorbent for effective removal of methyl orange and eriochrome black-T from aqueous phase, Environ Sci Pollut Res Int 25 (2018) 34319–34331, https://doi.org/10.1007/s11356-018-3367-2.
[99] R. Deng, D. Huang, J. Wan, W. Xue, L. Lei, X. Wen, et al., Chloro-phosphate impregnated biochar prepared by co-precipitation for the lead, cadmium and copper synergic scavenging from aqueous solution, Bioresour Technol 293 (2019), 122102, https://doi.org/10.1016/j.biortech.2019.122102.
[100] S. Shivalkar, P.K. Gautam, A. Verma, K. Maurya, M.P. Sk, S.K. Samanta, et al., Autonomous magnetic microbots for environmental remediation developed by organic waste derived carbon dots, J Environ Manage 297 (2021), 113322, https://doi.org/10.1016/j.jenvman.2021.113322.

[101] H. Zhao, Y. Lang, Adsorption behaviors and mechanisms of florfenicol by magnetic functionalized biochar and reed biochar, J Taiwan Inst Chem Eng 88 (2018) 152–160, https://doi.org/10.1016/j.jtice.2018.03.049.
[102] Q. Yang, X. Wang, W. Luo, J. Sun, Q. Xu, F. Chen, et al., Effectiveness and mechanisms of phosphate adsorption on iron-modified biochars derived from waste activated sludge, Bioresour Technol 247 (2018) 537–544, https://doi.org/10.1016/j.biortech.2017.09.136.
[103] B. Konkena, K. Junge Puring, I. Sinev, S. Piontek, O. Khavryuchenko, J.P. Durholt, et al., Pentlandite rocks as sustainable and stable efficient electrocatalysts for hydrogen generation, Nat Commun 7 (2016), 12269, https://doi.org/10.1038/ncomms12269.
[104] B. Szczęśniak, J. Choma, M. Jaroniec, Recent advances in mechanochemical synthesis of mesoporous metal oxides, Mater Adv 2 (2021) 2510–2523, https://doi.org/10.1039/D1MA00073J.
[105] A.P. Amrute, J. De Bellis, M. Felderhoff, F. Schuth, Mechanochemical synthesis of catalytic materials, Chemistry 27 (2021) 6819–6847, https://doi.org/10.1002/chem.202004583.
[106] M. Naghdi, M. Taheran, S.K. Brar, T. Rouissi, M. Verma, R.Y. Surampalli, et al., A green method for production of nanobiochar by ball milling-optimization and characterization, J Clean Prod 164 (2017) 1394–1405, https://doi.org/10.1016/j.jclepro.2017.07.084.
[107] J. Wu, J. Yang, G. Huang, C. Xu, B. Lin, Hydrothermal carbonization synthesis of cassava slag biochar with excellent adsorption performance for Rhodamine B, J Cleaner Prod 251 (2020) 119717, https://doi.org/10.1016/j.jclepro.2019.119717.
[108] O.M. Rodriguez-Narvaez, J.M. Peralta-Hernandez, A. Goonetilleke, E.R. Bandala, Biochar-supported nanomaterials for environmental applications, J Ind Eng Chem 78 (2019) 21–33, https://doi.org/10.1016/j.jiec.2019.06.008.
[109] D. Shan, S. Deng, T. Zhao, B. Wang, Y. Wang, J. Huang, et al., Preparation of ultrafine magnetic biochar and activated carbon for pharmaceutical adsorption and subsequent degradation by ball milling, J Hazard Mater 305 (2016) 156–163, https://doi.org/10.1016/j.jhazmat.2015.11.047.
[110] J. Hao, X. Meng, S. Fang, H. Cao, W. Lv, X. Zheng, et al., MnO_2-Functionalized amorphous carbon sorbents from spent lithium-ion batteries for highly efficient removal of cadmium from aqueous solutions, Ind Eng Chem Res 59 (2020) 10210–10220, https://doi.org/10.1021/acs.iecr.9b06670.
[111] R. Zheng, H. Gao, Z. Ren, D. Cen, Z. Chen, Preparation of activated bentonite and its adsorption behavior on oil-soluble green pigment, Physicochem Probl Miner Process 53 (2017) 829–845, https://doi.org/10.5277/ppmp170213.
[112] B.J. Ni, Q.S. Huang, C. Wang, T.Y. Ni, J. Sun, W. Wei, Competitive adsorption of heavy metals in aqueous solution onto biochar derived from anaerobically digested sludge, Chemosphere 219 (2019) 351–357, https://doi.org/10.1016/j.chemosphere.2018.12.053.
[113] M. Xu, P. Hadi, G. Chen, G. McKay, Removal of cadmium ions from wastewater using innovative electronic waste-derived material, J Hazard Mater 273 (2014) 118–123, https://doi.org/10.1016/j.jhazmat.2014.03.037.
[114] L. Liu, Y. Huang, S. Zhang, Y. Gong, Y. Su, J. Cao, et al., Adsorption characteristics and mechanism of Pb(II) by agricultural waste-derived biochars produced from a pilot-scale pyrolysis system, Waste Manage 100 (2019) 287–295, https://doi.org/10.1016/j.wasman.2019.08.021.
[115] Q. Zeng, S. Li, W. Sun, L. Hu, H. Zhong, Z. He, Eco-friendly leaching of rubidium from biotite-containing minerals with oxalic acid and effective removal of Hg^{2+} from aqueous solution using the leaching residues, J Clean Prod 306 (2021), 127167, https://doi.org/10.1016/j.jclepro.2021.127167.
[116] J. Hou, Y. Liu, S. Wen, W. Li, R. Liao, L. Wang, Sorghum-waste-derived high-surface area KOH-activated porous carbon for highly efficient methylene blue and Pb(II) removal, ACS Omega 5 (2020) 13548–13556, https://doi.org/10.1021/acsomega.9b04452.
[117] Y. Zhu, X. Wang, Z. Li, Y. Fan, X. Zhang, J. Chen, et al., Husbandry waste derived coralline-like composite biomass material for efficient heavy metal ions removal, Bioresour Technol 337 (2021), 125408, https://doi.org/10.1016/j.biortech.2021.125408.
[118] M.M. Ibrahim, H.S. El-Sheshtawy, A. El-Magied, O. Mahmoud, E.-S.A. Manaa, M.A. Youssef, et al., A facile and cost-effective adsorbent derived from industrial iron-making slag for uranium removal, J Radioanal Nucl Chem 329 (2021) 1291–1300, https://doi.org/10.1007/s10967-021-07914-6.
[119] K. Vijayaraghavan, R. Balasubramanian, Application of pinewood waste-derived biochar for the removal of nitrate and phosphate from single and binary solutions, Chemosphere 278 (2021), 130361, https://doi.org/10.1016/j.chemosphere.2021.130361.
[120] S. Mukherjee, B. Kamila, S. Paul, B. Hazra, S. Chowdhury, G. Halder, Optimizing fluoride uptake influencing parameters of paper industry waste derived activated carbon, Microchem J 160 (2021), 105643, https://doi.org/10.1016/j.microc.2020.105643.
[121] H. Hu, B. Jiang, J. Zhang, X. Chen, Adsorption of perrhenate ion by bio-char produced from Acidosasa edulis shoot shell in aqueous solution, RSC Adv 5 (2015) 104769–104778, https://doi.org/10.1039/C5RA20235C.
[122] C. Akmil-Başar, Y. Önal, T. Kılıçer, D. Eren, Adsorptions of high concentration malachite green by two activated carbons having different porous structures, J Hazard Mater 127 (2005) 73–80, https://doi.org/10.1016/j.jhazmat.2005.06.025.
[123] L. Ding, B. Zou, W. Gao, Q. Liu, Z. Wang, Y. Guo, et al., Adsorption of Rhodamine-B from aqueous solution using treated rice husk-based activated carbon, Colloids Surf, A 446 (2014) 1–7, https://doi.org/10.1016/j.colsurfa.2014.01.030.
[124] A. Jain, V. Gupta, A. Bhatnagar, Suhas, A comparative study of adsorbents prepared from industrial wastes for removal of dyes, Sep Sci Technol 38 (2003) 463–481, https://doi.org/10.1081/SS-120016585.
[125] H.T. Van, L.H. Nguyen, N.V. Dang, H.-P. Chao, Q.T. Nguyen, T.H. Nguyen, et al., The enhancement of reactive red 24 adsorption from aqueous solution using agricultural waste-derived biochar modified with ZnO nanoparticles, RSC Adv 11 (2021) 5801–5814, https://doi.org/10.1039/D0RA09974K.
[126] A. Gupta, A. Garg, Utilisation of sewage sludge derived adsorbents for the removal of recalcitrant compounds from wastewater: mechanistic aspects, isotherms, kinetics and thermodynamics, Bioresour Technol 194 (2015) 214–224, https://doi.org/10.1016/j.biortech.2015.07.005.
[127] K.-W. Jung, J.-H. Kim, J.-W. Choi, Synthesis of magnetic porous carbon composite derived from metal-organic framework using recovered terephthalic acid from polyethylene terephthalate (PET) waste bottles as organic ligand and its potential as adsorbent for antibiotic tetracycline hydrochloride, Composites, Part B 187 (2020) 107867, https://doi.org/10.1016/j.compositesb.2020.107867.
[128] S.-H. Chang, C.-C. Lu, C.-W. Lin, K.-S. Wang, M.-W. Lee, S.-H. Liu, Waste expanded polystyrene modified with H_2SO_4/biodegradable chelating agent for reuse: as a highly efficient adsorbent to remove fluoroquinolone antibiotic from water, Chemosphere 288 (2022), 132619, https://doi.org/10.1016/j.chemosphere.2021.132619.
[129] S. Teixeira, C. Delerue-Matos, L. Santos, Application of experimental design methodology to optimize antibiotics removal by walnut shell based activated carbon, Sci Total Environ 646 (2019) 168–176, https://doi.org/10.1016/j.scitotenv.2018.07.204.
[130] X.-R. Jing, Y.-Y. Wang, W.-J. Liu, Y.-K. Wang, H. Jiang, Enhanced adsorption performance of tetracycline in aqueous solutions by methanol-modified biochar, Chem Eng J 248 (2014) 168–174, https://doi.org/10.1016/j.cej.2014.03.006.
[131] Q. Zeng, H. Zhong, Z. He, L. Hu, Efficient removal of arsenite by a composite of amino modified silica supported MnO_2/Fe–Al hydroxide (SNMFA) prepared from biotite, J Environ Manage 291 (2021), 112678, https://doi.org/10.1016/j.jenvman.2021.112678.
[132] L. Ramrakhiani, S. Ghosh, S. Majumdar, Heavy metal recovery from electroplating effluent using adsorption by jute waste-derived biochar for soil amendment and plant micro-fertilizer, Clean Technol Environ Policy (2022) 1–24, https://doi.org/10.1007/s10098-021-02243-4.
[133] Z. Chen, R. Zheng, W. Wei, W. Wei, W. Zou, J. Li, et al., Recycling spent water treatment adsorbents for efficient electrocatalytic water oxidation reaction, Resour, Conserv Recycl 178 (2022), 106037, https://doi.org/10.1016/j.resconrec.2021.106037.
[134] W.W. Ngah, M.M. Hanafiah, Removal of heavy metal ions from wastewater by chemically modified plant wastes as adsorbents: a review, Bioresour Technol 99 (2008) 3935–3948, https://doi.org/10.1016/j.biortech.2007.06.011.
[135] Y. Liu, X. Zhang, J. Wang, A critical review of various adsorbents for selective removal of nitrate from water: structure, performance and mechanism, Chemosphere 291 (2022), 132728, https://doi.org/10.1016/j.chemosphere.2021.132728.
[136] J. Pan, B. Gao, W. Song, X. Xu, Q. Yue, Modified biogas residues as an eco-friendly and easily-recoverable biosorbent for nitrate and phosphate removals from surface water, J Hazard Mater 382 (2020), 121073, https://doi.org/10.1016/j.jhazmat.2019.121073.
[137] R. Qiu, F. Cheng, H. Huang, Removal of Cd^{2+} from aqueous solution using hydrothermally modified circulating fluidized bed fly ash resulting from coal gangue power plant, J Cleaner Prod 172 (2018) 1918–1927, https://doi.org/10.1016/j.jclepro.2017.11.236.
[138] L. Yang, T. Wen, L. Wang, T. Miki, H. Bai, X. Lu, et al., The stability of the compounds formed in the process of removal Pb(II), Cu(II) and Cd(II) by steelmaking slag in an acidic aqueous solution, J Environ Manage 231 (2019) 41–48, https://doi.org/10.1016/j.jenvman.2018.10.028.
[139] W. Zou, X. Feng, R. Wang, W. Wei, S. Luo, R. Zheng, et al., High-efficiency core-shell magnetic heavy-metal absorbents derived from spent-$LiFePO_4$ Battery, J Hazard Mater 402 (2021), 123583, https://doi.org/10.1016/j.jhazmat.2020.123583.
[140] L. Panda, S.S. Rath, D.S. Rao, B.B. Nayak, B. Das, P.K. Misra, Thorough understanding of the kinetics and mechanism of heavy metal adsorption onto a pyrophyllite mine waste based geopolymer, J Mol Liq 263 (2018) 428–441, https://doi.org/10.1016/j.molliq.2018.05.016.
[141] S. Pérez, J. Muñoz-Saldaña, J.A. Garcia-Nunez, N. Acelas, E. Flórez, Unraveling the Ca–P species produced over the time during phosphorus removal from aqueous solution using biocomposite of eggshell-palm mesocarp fiber, Chemosphere 287 (2022), 132333, https://doi.org/10.1016/j.chemosphere.2021.132333.
[142] N. Agasti, Decontamination of heavy metal ions from water by composites prepared from waste, Curr Res Green Sustain Chem 4 (2021), 100088, https://doi.org/10.1016/j.crgsc.2021.100088.
[143] Z. Li, L. Wang, J. Meng, X. Liu, J. Xu, F. Wang, et al., Zeolite-supported nanoscale zero-valent iron: new findings on simultaneous adsorption of Cd(II), Pb(II), and As(III) in aqueous solution and soil, J Hazard Mater 344 (2018) 1–11, https://doi.org/10.1016/j.jhazmat.2017.09.036.
[144] J. Han, G. Zhang, L. Zhou, F. Zhan, D. Cai, Z. Wu, Waste carton-derived nanocomposites for efficient removal of hexavalent chromium, Langmuir 34 (2018) 5955–5963, https://doi.org/10.1021/acs.langmuir.8b00225.
[145] A. Ngambia, J. Ifthikar, Shahib II, A. Jawad, A. Shahzad, M. Zhao, et al., Adsorptive purification of heavy metal contaminated wastewater with sewage

sludge derived carbon-supported Mg(II) composite, Sci Total Environ 691 (2019) 306–321, https://doi.org/10.1016/j.scitotenv.2019.07.003.
[146] W. Ouyang, X. Zhao, M. Tysklind, F. Hao, Typical agricultural diffuse herbicide sorption with agricultural waste-derived biochars amended soil of high organic matter content, Water Res 92 (2016) 156–163, https://doi.org/10.1016/j.watres.2016.01.055.
[147] T. Bao, M.M. Damtie, A. Hosseinzadeh, W. Wei, J. Jin, H.N. Phong Vo, et al., Bentonite-supported nano zero-valent iron composite as a green catalyst for bisphenol A degradation: preparation, performance, and mechanism of action, J Environ Manage 260 (2020), 110105, https://doi.org/10.1016/j.jenvman.2020.110105.
[148] Z. Chen, H. Gao, Y. Li, J. Jin, Z. Ren, W. Wang, Evaluation of sodium petroleum sulfonates with different molecular weights for flotation of kyanite ore, Physicochem Probl Miner Process 53 (2017) 956–968, https://doi.org/10.5277/ppmp170222.
[149] Z. Ren, Y. Shen, H. Gao, H. Chen, C. Liu, Z. Chen, Comparison of sodium oleate and sodium petroleum sulfonate for low-temperature flotation of fluorite and the collecting mechanisms, Mining, Metallurgy & Exploration 38 (2021) 2527–2536, https://doi.org/10.1007/s42461-021-00494-9.
[150] Z. Chen, Z. Ren, H. Gao, R. Zheng, Y. Jin, C. Niu, Flotation studies of fluorite and barite with sodium petroleum sulfonate and sodium hexametaphosphate, J Mater Res Technol 8 (2019) 1267–1273, https://doi.org/10.1016/j.jmrt.2018.10.002.
[151] Z. Chen, Z. Ren, H. Gao, Y. Qian, R. Zheng, Effect of modified starch on separation of fluorite from barite using sodium oleate, Physicochem Probl Miner Process 54 (2018) 228–237, https://doi.org/10.5277/ppmp1806.
[152] O. Paunovic, S. Pap, S. Maletic, M.A. Taggart, N. Boskovic, M.T. Sekulic, Ionisable emerging pharmaceutical adsorption onto microwave functionalised biochar derived from novel lignocellulosic waste biomass, J Colloid Interface Sci 547 (2019) 350–360, https://doi.org/10.1016/j.jcis.2019.04.011.
[153] F. Feizi, F. Reguyal, N. Antoniou, A. Zabaniotou, A.K. Sarmah, Environmental remediation in circular economy: end of life tyre magnetic pyrochars for adsorptive removal of pharmaceuticals from aqueous solution, Sci Total Environ 739 (2020), 139855, https://doi.org/10.1016/j.scitotenv.2020.139855.
[154] D. Bahamon, L.F. Vega, Pharmaceutical removal from water effluents by adsorption on activated carbons: a Monte Carlo simulation study, Langmuir 33 (2017) 11146–11155, https://doi.org/10.1021/acs.langmuir.7b01967.
[155] P. Joshi, O.P. Sharma, S.K. Ganguly, M. Srivastava, O.P. Khatri, Fruit waste-derived cellulose and graphene-based aerogels: plausible adsorption pathways for fast and efficient removal of organic dyes, J Colloid Interface Sci 608 (2022) 2870–2883, https://doi.org/10.1016/j.jcis.2021.11.016.
[156] M.S. Alivand, M. Najmi, N.H.M.H. Tehrani, A. Kamali, O. Tavakoli, A. Rashidi, et al., Tuning the surface chemistry and porosity of waste-derived nanoporous materials toward exceptional performance in antibiotic adsorption: experimental and DFT studies, Chem Eng J 374 (2019) 274–291, https://doi.org/10.1016/j.cej.2019.05.188.
[157] R. Guo, H. Liu, K. Yang, S. Wang, P. Sun, H. Gao, et al., β-Cyclodextrin polymerized in cross-flowing channels of biomass sawdust for rapid and highly efficient pharmaceutical pollutants removal from water, ACS Appl Mater Interfaces 12 (2020) 32817–32826, https://doi.org/10.1021/acsami.0c08729.
[158] G. Jaria, V. Calisto, M.V. Gil, P. Ferreira, S.M. Santos, M. Otero, et al., Effects of thiol functionalization of a waste-derived activated carbon on the adsorption of sulfamethoxazole from water: kinetic, equilibrium and thermodynamic studies, J Mol Liq 323 (2021), 115003, https://doi.org/10.1016/j.molliq.2020.115003.
[159] G. Jaria, M.A. Lourenço, C.P. Silva, P. Ferreira, M. Otero, V. Calisto, et al., Effect of the surface functionalization of a waste-derived activated carbon on pharmaceuticals' adsorption from water, J Mol Liq 299 (2020), 112098, https://doi.org/10.1016/j.molliq.2019.112098.
[160] P. Srinivasan, A.K. Sarmah, Characterisation of agricultural waste-derived biochars and their sorption potential for sulfamethoxazole in pasture soil: a spectroscopic investigation, Sci Total Environ 502 (2015) 471–480, https://doi.org/10.1016/j.scitotenv.2014.09.048.
[161] S. Wei, A.R. Kamali, Waste plastic derived Co_3Fe_7/$CoFe_2O_4$@carbon magnetic nanostructures for efficient dye adsorption, J Alloys Compd 886 (2021), 161201, https://doi.org/10.1016/j.jallcom.2021.161201.
[162] M. Ahmad, A.R. Usman, M.I. Rafique, M.I. Al-Wabel, Engineered biochar composites with zeolite, silica, and nano-zerovalent iron for the efficient scavenging of chlortetracycline from aqueous solutions, Environ Sci Pollut Res 26 (2019) 15136–15152, https://doi.org/10.1007/s11356-019-04850-7.
[163] A. Ashiq, B. Sarkar, N. Adassooriya, J. Walpita, A.U. Rajapaksha, Y.S. Ok, et al., Sorption process of municipal solid waste biochar-montmorillonite composite for ciprofloxacin removal in aqueous media, Chemosphere 236 (2019), 124384, https://doi.org/10.1016/j.chemosphere.2019.124384.
[164] P.S. Murphin Kumar, S. Ganesan, A.a.H. Al-Muhtaseb, L. Al-Haj, M. Elancheziyan, S. Shobana, et al., Tropical fruit waste-derived mesoporous rock-like Fe_2O_3/C composite fabricated with amphiphilic surfactant-templating approach showing massive potential for high-tech applications, Int J Energy Res 45 (2021) 17417–17430, https://doi.org/10.1002/er.6798.
[165] Y. Mei, J. Xu, Y. Zhang, B. Li, S. Fan, H. Xu, Effect of Fe-N modification on the properties of biochars and their adsorption behavior on tetracycline removal from aqueous solution, Bioresour Technol 325 (2021), 124732, https://doi.org/10.1016/j.biortech.2021.124732.
[166] A.A. Basaleh, M.H. Al-Malack, T.A. Saleh, Poly (acrylamide acrylic acid) grafted on steel slag as an efficient magnetic adsorbent for cationic and anionic dyes, J Environ Chem Eng 9 (2021), 105126, https://doi.org/10.1016/j.jece.2021.105126.
[167] J. Li, W. Pan, Q. Liu, Z. Chen, Z. Chen, X. Feng, et al., Interfacial engineering of $Bi_{19}Br_3S_{27}$ nanowires promotes metallic photocatalytic CO_2 reduction activity under near-infrared light irradiation, J Am Chem Soc 143 (2021) 6551–6559, https://doi.org/10.1021/jacs.1c01109.
[168] X. Liu, X. Duan, T. Bao, D. Hao, Z. Chen, W. Wei, et al., High-performance photocatalytic decomposition of PFOA by BiOX/TiO_2 heterojunctions: self-induced inner electric fields and band Alignment, J Hazard Mater (2022), 128195, https://doi.org/10.1016/j.jhazmat.2021.128195.
[169] X. Liu, Z. Chen, K. Tian, F. Zhu, D. Hao, D. Cheng, et al., Fe^{3+} promoted the photocatalytic defluorination of perfluorooctanoic acid (PFOA) over In_2O_3, ACS ES&T Water 1 (2021) 2431–2439, https://doi.org/10.1021/acsestwater.1c00275.
[170] D. Hao, C. Liu, X. Xu, M. Kianinia, I. Aharonovich, X. Bai, et al., Surface defect-abundant one-dimensional graphitic carbon nitride nanorods boost photocatalytic nitrogen fixation, New J Chem 44 (2020) 20651–20658, https://doi.org/10.1039/D0NJ04068A.
[171] M. Ma, Y. Liu, Y. Wei, D. Hao, W. Wei, B.-J. Ni, A facile oxygen vacancy and bandgap control of Bi(OH)SO_4·H_2O for achieving enhanced photocatalytic remediation, J Environ Manage 294 (2021), 113046, https://doi.org/10.1016/j.jenvman.2021.113046.
[172] X. Liu, B. Xu, X. Duan, Q. Hao, W. Wei, S. Wang, et al., Facile preparation of hydrophilic in $_2O_3$ nanospheres and rods with improved performances for photocatalytic degradation of PFOA, Environ Sci: Nano 8 (2021) 1010–1018, https://doi.org/10.1039/D0EN01216E.
[173] K. Shirvanimoghaddam, B. Czech, G. Wójcik, M. Naebe, The light enhanced removal of Bisphenol A from wastewater using cotton waste derived carbon microtubes, J Colloid Interface Sci 539 (2019) 425–432, https://doi.org/10.1016/j.jcis.2018.12.090.
[174] P.K. Boruah, A. Yadav, M.R. Das, Magnetic mixed metal oxide nanomaterials derived from industrial waste and its photocatalytic applications in environmental remediation, J Environ Chem Eng 8 (2020), 104297, https://doi.org/10.1016/j.jece.2020.104297.
[175] S. Babar, N. Gavade, H. Shinde, A. Gore, P. Mahajan, K.H. Lee, et al., An innovative transformation of waste toner powder into magnetic g-C_3N_4-Fe_2O_3 photocatalyst: sustainable e-waste management, J Environ Chem Eng 7 (2019), 103041, https://doi.org/10.1016/j.jece.2019.103041.
[176] W. Zhang, Z. Liu, C. Xu, W. He, G. Li, J. Huang, et al., Preparing graphene oxide–copper composite material from spent lithium ion batteries and catalytic performance analysis, Res Chem Intermed 44 (2018) 5075–5089, https://doi.org/10.1007/s11164-018-3410-4.
[177] M. Hojamberdiev, B. Czech, A. Wasilewska, A. Boguszewska-Czubara, K. Yubuta, H. Wagata, et al., Detoxifying SARS-CoV-2 antiviral drugs from model and real wastewaters by industrial waste-derived multiphase photocatalysts, J Hazard Mater 429 (2022), 128300, https://doi.org/10.1016/j.jhazmat.2022.128300.
[178] J. Loke, R.M. Zaki, H. Setiabudi, Photocatalytic degradation of methylene blue using ZnO supported on wood waste-derived activated carbon (ZnO/AC), Mater Today: Proc (2022), https://doi.org/10.1016/j.matpr.2021.12.535.
[179] E.C. Umejuru, E. Prabakaran, K. Pillay, Coal fly ash coated with carbon hybrid nanocomposite for remediation of cadmium(II) and photocatalytic application of the spent adsorbent for reuse, Results Mater 7 (2020), 100117, https://doi.org/10.1016/j.rinma.2020.100117.
[180] E.C. Umejuru, E. Prabakaran, K. Pillay, Coal fly ash decorated with graphene oxide–tungsten oxide nanocomposite for rapid removal of Pb^{2+} ions and reuse of spent adsorbent for photocatalytic degradation of acetaminophen, ACS Omega 6 (2021) 11155–11172, https://doi.org/10.1021/acsomega.0c04194.
[181] İ. Altın, M. Sökmen, Photocatalytic properties of silver incorporated titania nanoparticles immobilized on waste-derived polystyrene, Water, Air, Soil Pollut 225 (2014) 1–12, https://doi.org/10.1007/s11270-013-1786-8.
[182] D.M. Abdo, S.M. Abdelbasir, S.T. El-Sheltawy, I.A. Ibrahim, Recovery of Tin as Tin oxide nanoparticles from waste printed circuit boards for photocatalytic dye degradation, Korean J Chem Eng 38 (2021) 1934–1945, https://doi.org/10.1007/s11814-021-0838-9.
[183] A. Amarasinghe, D. Wanniarachchi, Eco-friendly photocatalyst derived from egg shell waste for dye degradation, J Chem 2019 (2019), 8184732, https://doi.org/10.1155/2019/8184732.
[184] F. Mohamed, M. Shaban, G. Aljohani, A.M. Ahmed, Synthesis of novel eco-friendly CaO/C photocatalyst from coffee and eggshell wastes for dye degradation, J Mater Res Technol 14 (2021) 3140–3149, https://doi.org/10.1016/j.jmrt.2021.08.055.
[185] C.V. Montoya-Bautista, P. Acevedo-Peña, R. Zanella, R.-M. Ramírez-Zamora, Characterization and evaluation of copper slag as a bifunctional photocatalyst for alcohols degradation and hydrogen production, Top Catal 64 (2021) 131–141, https://doi.org/10.1007/s11244-020-01362-4.
[186] H.-C. Yang, M.-T. Liu, M.-W. Chao, K.-H. Wang, C. Hu, Polymeric g-C_3N_4 derived from the mixture of dicyandiamide and mushroom waste for photocatalytic degradation of methyl blue, Top Catal 63 (2020) 1182–1192, https://doi.org/10.1007/s11244-020-01237-8.
[187] P. Khare, A. Singh, S. Verma, A. Bhati, A.K. Sonker, K.M. Tripathi, et al., Sunlight-induced selective photocatalytic degradation of methylene blue in bacterial culture by pollutant soot derived nontoxic graphene nanosheets, ACS Sustainable Chem Eng 6 (2018) 579–589, https://doi.org/10.1021/acssuschemeng.7b02929.
[188] R. Aggarwal, D. Saini, B. Singh, J. Kaushik, A.K. Garg, S.K. Sonkar, Bitter apple peel derived photoactive carbon dots for the sunlight induced photocatalytic degradation of crystal violet dye, Solar Energy 197 (2020) 326–331, https://doi.org/10.1016/j.solener.2020.01.010.
[189] R. Aggarwal, D. Saini, S.K. Sonkar, A.K. Sonker, G. Westman, Sunlight promoted removal of toxic hexavalent chromium by cellulose derived photoactive carbon

dots, Chemosphere 287 (2022), 132287, https://doi.org/10.1016/j.chemosphere.2021.132287.
[190] D. Monje, K. Chacon, I. Galindo, C. Castaño, L. Ballesteros-Rueda, G. Valencia, et al., Carbon dots from agroindustrial residues: a critical comparison of the effect of physicochemical properties on their performance as photocatalyst and emulsion stabilizer, Mater Today Chem 20 (2021), 100445, https://doi.org/10.1016/j.mtchem.2021.100445.
[191] Z. Chen, X. Duan, W. Wei, S. Wang, B.-J. Ni, Iridium-based nanomaterials for electrochemical water splitting, Nano Energy 78 (2020), 105270, https://doi.org/10.1016/j.nanoen.2020.105270.
[192] Z. Chen, X. Duan, W. Wei, S. Wang, B.-J. Ni, Electrocatalysts for acidic oxygen evolution reaction: achievements and perspectives, Nano Energy 78 (2020), 105392, https://doi.org/10.1016/j.nanoen.2020.105392.
[193] Z. Chen, X. Duan, W. Wei, S. Wang, B.-J. Ni, Recent advances in transition metal-based electrocatalysts for alkaline hydrogen evolution, J Mater Chem A 7 (2019) 14971–15005, https://doi.org/10.1039/C9TA03220G.
[194] Z. Sun, X. Wu, K. Qu, Z. Huang, S. Liu, M. Dong, et al., Bimetallic metal-organic frameworks anchored corncob-derived porous carbon photocatalysts for synergistic degradation of organic pollutants, Chemosphere 259 (2020), 127389, https://doi.org/10.1016/j.chemosphere.2020.127389.
[195] S. Joseph, G. Saianand, M.R. Benzigar, K. Ramadass, G. Singh, A.I. Gopalan, et al., Recent advances in functionalized nanoporous carbons derived from waste resources and their applications in energy and environment, Adv Sustainable Syst 5 (2021), 2000169, https://doi.org/10.1002/adsu.202000169.
[196] S. Sekar, I. Rabani, C. Bathula, S. Kumar, S. Govindaraju, K. Yun, et al., Graphitic carbon-encapsulated V_2O_5 nanocomposites as a superb photocatalyst for crystal violet degradation, Environ Res (2021), 112201, https://doi.org/10.1016/j.envres.2021.112201.
[197] S. Luo, S. Li, S. Zhang, Z. Cheng, T.T. Nguyen, M. Guo, Visible-light-driven Z-scheme protonated g-C_3N_4/wood flour biochar/$BiVO_4$ photocatalyst with biochar as charge-transfer channel for enhanced RhB degradation and Cr(VI) reduction, Sci Total Environ 806 (2022), 150662, https://doi.org/10.1016/j.scitotenv.2021.150662.
[198] Q. Men, T. Wang, C. Ma, L. Yang, Y. Liu, P. Huo, et al., In-suit preparation of CdSe quantum dots/porous channel biochar for improving photocatalytic activity for degradation of tetracycline, J Taiwan Inst Chem Eng 99 (2019) 180–192, https://doi.org/10.1016/j.jtice.2019.03.019.
[199] W. Shi, H. Ren, X. Huang, M. Li, Y. Tang, F. Guo, Low cost red mud modified graphitic carbon nitride for the removal of organic pollutants in wastewater by the synergistic effect of adsorption and photocatalysis, Sep Purif Technol 237 (2020), 116477, https://doi.org/10.1016/j.seppur.2019.116477.
[200] Y. Zhai, Y. Dai, J. Guo, L. Zhou, M. Chen, H. Yang, et al., Novel biochar@$CoFe_2O_4$/Ag_3PO_4 photocatalysts for highly efficient degradation of bisphenol a under visible-light irradiation, J Colloid Interface Sci 560 (2020) 111–121, https://doi.org/10.1016/j.jcis.2019.08.065.
[201] X. Zhang, M. Liu, Z. Kang, B. Wang, B. Wang, F. Jiang, et al., NIR-triggered photocatalytic/photothermal/photodynamic water remediation using eggshell-derived $CaCO_3$/CuS nanocomposites, Chem Eng J 388 (2020), 124304, https://doi.org/10.1016/j.cej.2020.124304.
[202] K.O. Kassem, M.A. Hussein, M.M. Motawea, H. Gomaa, Z. Alrowaili, M. Ezzeldien, Design of mesoporous ZnO@silica fume-derived SiO_2 nanocomposite as photocatalyst for efficient crystal violet removal: effective route to recycle industrial waste, J Clean Prod 326 (2021), 129416, https://doi.org/10.1016/j.jclepro.2021.129416.
[203] M. Chowdhury, S. Shoko, F. Cummings, V. Fester, T.V. Ojumu, Charge transfer between biogenic jarosite derived Fe^{3+} and TiO_2 enhances visible light photocatalytic activity of TiO_2, J Environ Sci 54 (2017) 256–267, https://doi.org/10.1016/j.jes.2015.11.038.
[204] D. Kartikaningsih, Y.H. Huang, Y.J. Shih, Electro-oxidation and characterization of nickel foam electrode for removing boron, Chemosphere 166 (2017) 184–191, https://doi.org/10.1016/j.chemosphere.2016.09.091.
[205] W. Wei, X. Feng, R. Wang, R. Zheng, D. Yang, H. Chen, Electrochemical driven phase segregation enabled dual-ion removal battery deionization electrode, Nano Lett 21 (2021) 4830–4837, https://doi.org/10.1021/acs.nanolett.1c01487.
[206] G. Bharath, A. Hai, K. Rambabu, F. Ahmed, A.S. Haidyrah, N. Ahmad, et al., Hybrid capacitive deionization of NaCl and toxic heavy metal ions using faradic electrodes of silver nanospheres decorated pomegranate peel-derived activated carbon, Environ Res 197 (2021), 111110, https://doi.org/10.1016/j.envres.2021.111110.
[207] N. Deka, J. Barman, S. Kasthuri, V. Nutalapati, G.K. Dutta, Transforming waste polystyrene foam into N-doped porous carbon for capacitive energy storage and deionization applications, Appl Surf Sci 511 (2020), 145576, https://doi.org/10.1016/j.apsusc.2020.145576.
[208] H. Wang, T. Yan, J. Shen, J. Zhang, L. Shi, D. Zhang, Efficient removal of metal ions by capacitive deionization with straw waste derived graphitic porous carbon nanosheets, Environ Sci: Nano 7 (2020) 317–326, https://doi.org/10.1039/C9EN01233H.
[209] P. Li, T. Feng, Z. Song, Y. Tan, W. Luo, Chitin derived biochar for efficient capacitive deionization performance, RSC Adv 10 (2020) 30077–30086, https://doi.org/10.1039/D0RA05554A.
[210] Y.-H. Tang, S.-H. Liu, D.C. Tsang, Microwave-assisted production of CO_2-activated biochar from sugarcane bagasse for electrochemical desalination, J Hazard Mater 383 (2020), 121192, https://doi.org/10.1016/j.jhazmat.2019.121192.
[211] Q. Dong, D. Yang, L. Luo, Q. He, F. Cai, S. Cheng, et al., Engineering porous biochar for capacitive fluorine removal, Sep Purif Technol 257 (2021), 117932, https://doi.org/10.1016/j.seppur.2020.117932.
[212] S.-H. Liu, Y.-H. Tang, Hierarchically porous biocarbons prepared by microwave-aided carbonization and activation for capacitive deionization, J Electroanal Chem 878 (2020), 114587, https://doi.org/10.1016/j.jelechem.2020.114587.
[213] K. Shirvanimoghaddam, B. Czech, S. Abdikheibari, G. Brodie, M. Kończak, A. Krzyszczak, et al., Microwave synthesis of biochar for environmental applications, J Anal Appl Pyrolysis 161 (2021), 105415, https://doi.org/10.1016/j.jaap.2021.105415.
[214] G. Li, F. Yang, L. Wu, L. Qian, X. Hu, Z. Wang, et al., Agricultural waste buckwheat husk derived bifunctional nitrogen, sulfur and oxygen-co-doped porous carbon for symmetric supercapacitors and capacitive deionization, New J Chem 45 (2021) 10432–10447, https://doi.org/10.1039/D1NJ00579K.
[215] Z. Chen, R. Zheng, M. Grać, W. Wei, G. Lota, H. Chen, et al., Tuning electronic property and surface reconstruction of amorphous iron borides via W-P co-doping for highly efficient oxygen evolution, Appl Catal B 288 (2021) 120037, https://doi.org/10.1016/j.apcatb.2021.120037.
[216] Z. Chen, X. Duan, W. Wei, S. Wang, Z. Zhang, B.-J. Ni, Boride-based electrocatalysts: emerging candidates for water splitting, Nano Res 13 (2020) 293–314, https://doi.org/10.1007/s12274-020-2618-y.
[217] Y. Chang, Q. Dang, I. Samo, Y. Li, X. Li, G. Zhang, et al., Electrochemical heavy metal removal from water using PVC waste-derived N, S co-doped carbon materials, RSC Adv 10 (2020) 4064–4070, https://doi.org/10.1039/C9RA09237D.
[218] H. Stephanie, T.E. Mlsna, D.O. Wipf, Functionalized biochar electrodes for asymmetrical capacitive deionization, Desalination 516 (2021), 115240, https://doi.org/10.1016/j.desal.2021.115240.
[219] B. Wang, Y. Zhai, T. Hu, Q. Niu, S. Li, X. Liu, et al., Green quaternary ammonium nitrogen functionalized mesoporous biochar for sustainable electro-adsorption of perchlorate, Chem Eng J 419 (2021), 129585, https://doi.org/10.1016/j.cej.2021.129585.
[220] M.T.Z. Myint, J. Dutta, Fabrication of zinc oxide nanorods modified activated carbon cloth electrode for desalination of brackish water using capacitive deionization approach, Desalination 305 (2012) 24–30, https://doi.org/10.1016/j.desal.2012.08.010.
[221] Y.-H. Liu, H.-C. Hsi, K.-C. Li, C.-H. Hou, Electrodeposited manganese dioxide/activated carbon composite as a high-performance electrode material for capacitive deionization, ACS Sustainable Chem Eng 4 (2016) 4762–4770, https://doi.org/10.1021/acssuschemeng.6b00974.
[222] J. Adorna Jr., M. Borines, R.-A. Doong, Coconut shell derived activated biochar–manganese dioxide nanocomposites for high performance capacitive deionization, Desalination 492 (2020), 114602, https://doi.org/10.1016/j.desal.2020.114602.
[223] G. Bharath, K. Rambabu, F. Banat, A. Hai, A.F. Arangadi, N. Ponpandian, Enhanced electrochemical performances of peanut shell derived activated carbon and its Fe_3O_4 nanocomposites for capacitive deionization of Cr(VI) ions, Sci Total Environ 691 (2019) 713–726, https://doi.org/10.1016/j.scitotenv.2019.07.069.
[224] K. Rambabu, G. Bharath, A. Hai, S. Luo, K. Liao, M.A. Haija, et al., Development of watermelon rind derived activated carbon/manganese ferrite nanocomposite for cleaner desalination by capacitive deionization, J Clean Prod 272 (2020), 122626, https://doi.org/10.1016/j.envres.2021.111110.
[225] Y. Liu, X. Zhang, X. Gu, N. Wu, R. Zhang, Y. Shen, et al., One-step turning leather wastes into heteroatom doped carbon aerogel for performance enhanced capacitive deionization, Microporous Mesoporous Mater 303 (2020), 110303, https://doi.org/10.1016/j.micromeso.2020.110303.
[226] P.T. Juchen, K.M. Barcelos, K.S. Oliveira, L.A. Ruotolo, Using crude residual glycerol as precursor of sustainable activated carbon electrodes for capacitive deionization desalination, Chem Eng J 429 (2022), 132209, https://doi.org/10.1016/j.cej.2021.132209.
[227] J. Weng, S. Wang, G. Wang, P. Zhang, B. Lu, J. Jiang, et al., One-step activation of anode materials from spent lithium-ion batteries as high-performance electrodes for capacitive deionization, ChemElectroChem 8 (2021) 370–376, https://doi.org/10.1002/celc.202001417.
[228] T. Zhang, J. Xu, J. Qian, J. Zhang, The spent FCC catalyst loaded with Sb-doped SnO_2 and its application in electrocatalytic degradation of methylene blue, J Mater Sci 55 (2020) 13605–13617, https://doi.org/10.1007/s10853-020-04998-5.
[229] A. Petala, G. Bampos, Z. Frontistis, Using sawdust derived biochar as a novel 3D particle electrode for micropollutants degradation, Water 14 (2022) 357, https://doi.org/10.3390/w14030357.
[230] Q. Liu, S. Jiang, X. Su, X. Zhang, W. Cao, Y. Xu, Role of the biochar modified with $ZnCl_2$ and $FeCl_3$ on the electrochemical degradation of nitrobenzene, Chemosphere 275 (2021), 129966, https://doi.org/10.1016/j.chemosphere.2021.129966.
[231] Z. Chen, W. Wei, L. Song, B.-J. Ni, Hybrid water electrolysis: a new sustainable avenue for energy-saving hydrogen production, Sustainable Horizons 1 (2022), 100002, https://doi.org/10.1016/j.horiz.2021.100002.
[232] Z. Chen, R. Zheng, W. Wei, W. Wei, B.-J. Ni, H. Chen, Unlocking the electrocatalytic activity of natural chalcopyrite using mechanochemistry, J Energy Chem 68 (2022) 275–283, https://doi.org/10.1016/j.jechem.2021.11.005.
[233] Z. Chen, I. Ibrahim, D. Hao, X. Liu, L. Wu, W. Wei, et al., Controllable design of nanoworm-like nickel sulfides for efficient electrochemical water splitting in alkaline media, Mater, Today Energy 18 (2020), 100573, https://doi.org/10.1016/j.mtener.2020.100573.
[234] Y. Wang, C. Cui, G. Zhang, Y. Xin, S. Wang, Electrocatalytic hydrodechlorination of pentachlorophenol on Pd-supported magnetic biochar particle electrodes, Sep Purif Technol 258 (2021), 118017, https://doi.org/10.1016/j.seppur.2020.118017.

[235] Y. Wang, X. Tian, S. Wang, C. Cui, Y. Xin, G. Zhang, et al., In situ-synthesized amorphous Pd/NC microspheres derived from shrimp shells as a three-dimensional electrocatalyst for hydrodechlorination of diclofenac, Chem Eng J 428 (2022), 131231, https://doi.org/10.1016/j.cej.2021.131231.
[236] Y. Gong, J. Wan, P. Zhou, X. Wang, J. Chen, K. Xu, Oxygen and nitrogen-enriched hierarchical MoS_2 nanospheres decorated cornstalk-derived activated carbon for electrocatalytic degradation and supercapacitors, Mater Sci Semicond Process 123 (2021), 105533, https://doi.org/10.1016/j.mssp.2020.105533.
[237] Y. Zhao, X. Qiu, Z. Ma, C. Zhao, Z. Li, S. Zhai, Fabrication of Pd/Sludge-biochar electrode with high electrochemical activity on reductive degradation of 4-chlorophenol in wastewater, Environ Res (2022), 112740, https://doi.org/10.1016/j.envres.2022.112740.
[238] F. Yao, Q. Yang, M. Yan, X. Li, F. Chen, Y. Zhong, et al., Synergistic adsorption and electrocatalytic reduction of bromate by Pd/N-doped loofah sponge-derived biochar electrode, J Hazard Mater 386 (2020), 121651, https://doi.org/10.1016/j.jhazmat.2019.121651.
[239] T. Zhang, Y. Liu, L. Yang, W. Li, W. Wang, P. Liu, Ti–Sn–Ce/bamboo biochar particle electrodes for enhanced electrocatalytic treatment of coking wastewater in a three-dimensional electrochemical reaction system, J Clean Prod 258 (2020), 120273, https://doi.org/10.1016/j.jclepro.2020.120273.
[240] J. Ji, X.-Y. Li, J. Xu, X.-Y. Yang, H.-S. Meng, Z.-R. Yan, Zn-Fe-rich granular sludge carbon (GSC) for enhanced electrocatalytic removal of bisphenol A (BPA) and Rhodamine B (RhB) in a continuous-flow three-dimensional electrode reactor (3DER), Electrochim Acta 284 (2018) 587–596, https://doi.org/10.1016/j.electacta.2018.07.203.
[241] W. Wu, S. Zhu, X. Huang, W. Wei, B.-J. Ni, Mechanisms of persulfate activation on biochar derived from two different sludges: dominance of their intrinsic compositions, J Hazard Mater 408 (2021), 124454, https://doi.org/10.1016/j.jhazmat.2020.124454.
[242] Y. Yao, H. Chen, C. Lian, F. Wei, D. Zhang, G. Wu, et al., Fe, Co, Ni nanocrystals encapsulated in nitrogen-doped carbon nanotubes as Fenton-like catalysts for organic pollutant removal, J Hazard Mater 314 (2016) 129–139, https://doi.org/10.1016/j.jhazmat.2016.03.089.
[243] Z. Wu, Y.-Y. Gu, S. Xin, L. Lu, Z. Huang, M. Li, et al., Cu_xNi_yCo-LDH nanosheets on graphene oxide: an efficient and stable Fenton-like catalyst for dual-mechanism degradation of tetracycline, Chem Eng J (2022), 134574, https://doi.org/10.1016/j.cej.2022.134574.
[244] Z. Jia, X. Duan, P. Qin, W. Zhang, W. Wang, C. Yang, et al., Disordered atomic packing structure of metallic glass: toward ultrafast hydroxyl radicals production rate and strong electron transfer ability in catalytic performance, Adv Funct Mater 27 (2017), 1702258, https://doi.org/10.1002/adfm.201702258.
[245] Y. Zhuang, X. Wang, L. Zhang, Z. Kou, B. Shi, Confinement Fenton-like degradation of perfluorooctanoic acid by a three dimensional metal-free catalyst derived from waste, Appl Catal B 275 (2020), 119101, https://doi.org/10.1016/j.apcatb.2020.119101.
[246] C. Wang, R. Sun, R. Huang, H. Wang, Superior fenton-like degradation of tetracycline by iron loaded graphitic carbon derived from microplastics: synthesis, catalytic performance, and mechanism, Sep Purif Technol 270 (2021), 118773, https://doi.org/10.1016/j.seppur.2021.118773.
[247] Q. Wang, Y. Ma, S. Xing, Comparative study of Cu-based bimetallic oxides for Fenton-like degradation of organic pollutants, Chemosphere 203 (2018) 450–456, https://doi.org/10.1016/j.chemosphere.2018.04.013.
[248] C. Wang, R. Sun, R. Huang, Highly dispersed iron-doped biochar derived from sawdust for Fenton-like degradation of toxic dyes, J Clean Prod 297 (2021), 126681, https://doi.org/10.1016/j.jclepro.2021.126681.
[249] L. Gao, L. Wang, S. Li, Y. Cao, Highly active Fenton-like catalyst derived from solid waste-iron ore tailings using wheat straw pyrolysis, Environ Sci Pollut Res (2022) 1–11, https://doi.org/10.1007/s11356-021-17168-0.
[250] Q. Gan, H. Hou, S. Liang, J. Qiu, S. Tao, L. Yang, et al., Sludge-derived biochar with multivalent iron as an efficient Fenton catalyst for degradation of 4-Chlorophenol, Sci Total Environ 725 (2020), 138299, https://doi.org/10.1016/j.scitotenv.2020.138299.
[251] G. Ye, J. Zhou, R. Huang, Y. Ke, Y. Peng, Y. Zhou, et al., Magnetic sludge-based biochar derived from Fenton sludge as an efficient heterogeneous Fenton catalyst for degrading Methylene blue, J Environ Chem Eng 10 (2022) 107242, https://doi.org/10.1016/j.jece.2022.107242.
[252] M.A. Ahsan, A.R.P. Santiago, A. Rodriguez, V. Maturano-Rojas, B. Alvarado-Tenorio, R. Bernal, et al., Biomass-derived ultrathin carbon-shell coated iron nanoparticles as high-performance tri-functional HER, ORR and Fenton-like catalysts, J Clean Prod 275 (2020), 124141, https://doi.org/10.1016/j.jclepro.2020.124141.
[253] C. Wang, Y. Cao, H. Wang, Copper-based catalyst from waste printed circuit boards for effective Fenton-like discoloration of Rhodamine B at neutral pH, Chemosphere 230 (2019) 278–285, https://doi.org/10.1016/j.chemosphere.2019.05.068.
[254] C. Zhou, H. Zhou, Y. Yuan, J. Peng, G. Yao, P. Zhou, et al., Coupling adsorption and in-situ Fenton-like oxidation by waste leather-derived materials in continuous flow mode towards sustainable removal of trace antibiotics, Chem Eng J 420 (2021), 130370, https://doi.org/10.1016/j.cej.2021.130370.
[255] L. Lyu, G. Yu, L. Zhang, C. Hu, Y. Sun, 4-phenoxyphenol-functionalized reduced graphene oxide nanosheets: a metal-free Fenton-like catalyst for pollutant destruction, Environ Sci Technol 52 (2018) 747–756, https://doi.org/10.1021/acs.est.7b04865.
[256] J.-H. Chu, J.-K. Kang, S.-J. Park, C.-G. Lee, Bisphenol A degradation using waste antivirus copper film with enhanced sono-Fenton-like catalytic oxidation, Chemosphere 276 (2021), 130218, https://doi.org/10.1016/j.chemosphere.2021.130218.
[257] J.-H. Chu, J.-K. Kang, S.-J. Park, C.-G. Lee, Enhanced sonocatalytic degradation of bisphenol A with a magnetically recoverable biochar composite using rice husk and rice bran as substrate, J Environ Chem Eng 9 (2021), 105284, https://doi.org/10.1016/j.jece.2021.105284.
[258] Z. Cheng, S. Luo, X. Li, S. Zhang, T.T. Nguyen, M. Guo, et al., Ultrasound-assisted heterogeneous Fenton-like process for methylene blue removal using magnetic $MnFe_2O_4$/biochar nanocomposite, Appl Surf Sci 566 (2021), 150654, https://doi.org/10.1016/j.apsusc.2021.150654.
[259] J.-H. Chu, J.-K. Kang, S.-J. Park, C.-G. Lee, Application of magnetic biochar derived from food waste in heterogeneous sono-Fenton-like process for removal of organic dyes from aqueous solution, J Water Process Eng 37 (2020), 101455, https://doi.org/10.1016/j.jwpe.2020.101455.
[260] I. Robles, G. Moreno-Rubio, J.D. García-Espinoza, C. Martínez-Sánchez, A. Rodríguez, Y. Meas-Vong, et al., Study of polarized activated carbon filters as simultaneous adsorbent and 3D-type electrode materials for electro-Fenton reactors, J Environ Chem Eng 8 (2020), 104414, https://doi.org/10.1016/j.jece.2020.104414.
[261] N. Nasuha, S. Ismail, B. Hameed, Activated electric arc furnace slag as an effective and reusable Fenton-like catalyst for the photodegradation of methylene blue and acid blue 29, J Environ Manage 196 (2017) 323–329, https://doi.org/10.1016/j.jenvman.2017.02.070.
[262] A. Rocha, L. Magnago, J. Santos, V. Leal, A. Marins, V. Pegoretti, et al., Copper ferrite synthesis from spent Li-ion batteries for multifunctional application as catalyst in photo Fenton process and as electrochemical pseudocapacitor, Mater Res Bull 113 (2019) 231–240, https://doi.org/10.1016/j.materresbull.2019.02.007.
[263] Y. Liu, X. Zheng, S. Zhang, S. Sun, Enhanced removal of ibuprofen by heterogeneous photo-Fenton-like process over sludge-based Fe_3O_4-MnO_2 catalysts, Water Sci Technol 85 (2022) 291–304, https://doi.org/10.2166/wst.2021.612.
[264] Y. Chen, R. Su, F. Wang, W. Zhou, B. Gao, Q. Yue, et al., In-situ synthesis of CuS@carbon nanocomposites and application in enhanced photo-fenton degradation of 2, 4-DCP, Chemosphere 270 (2021), 129295, https://doi.org/10.1016/j.chemosphere.2020.129295.
[265] F. Deng, H. Olvera-Vargas, O. Garcia-Rodriguez, Y. Zhu, J. Jiang, S. Qiu, et al., Waste-wood-derived biochar cathode and its application in electro-Fenton for sulfathiazole treatment at alkaline pH with pyrophosphate electrolyte, J Hazard Mater 377 (2019) 249–258, https://doi.org/10.1016/j.jhazmat.2019.05.077.
[266] Z. Cao, X. Zheng, H. Cao, H. Zhao, Z. Sun, Z. Guo, et al., Efficient reuse of anode scrap from lithium-ion batteries as cathode for pollutant degradation in electro-Fenton process: role of different recovery processes, Chem Eng J 337 (2018) 256–264, https://doi.org/10.1016/j.cej.2017.12.104.
[267] F. Deng, S. Li, M. Zhou, Y. Zhu, S. Qiu, K. Li, et al., A biochar modified nickel-foam cathode with iron-foam catalyst in electro-Fenton for sulfamerazine degradation, Appl Catal B 256 (2019), 117796, https://doi.org/10.1016/j.apcatb.2019.117796.
[268] Y. Zhu, C. Chen, M. Tian, Y. Chen, Y. Yang, S. Gao, Self-powered electro-Fenton degradation system using oxygen-containing functional groups-rich biomass-derived carbon catalyst driven by 3D printed flexible triboelectric nanogenerator, Nano Energy 83 (2021), 105720, https://doi.org/10.1016/j.nanoen.2020.105720.
[269] Y. Zhu, M. Tian, Y. Chen, Y. Yang, X. Liu, S. Gao, 3D printed triboelectric nanogenerator self-powered electro-Fenton degradation of orange IV and crystal violet system using N-doped biomass carbon catalyst with tunable catalytic activity, Nano Energy 83 (2021), 105824, https://doi.org/10.1016/j.nanoen.2021.105824.
[270] W. Zhou, F. Li, Y. Su, J. Li, S. Chen, L. Xie, et al., O-doped graphitic granular biochar enables pollutants removal via simultaneous H_2O_2 generation and activation in neutral Fe-free electro-Fenton process, Sep Purif Technol 262 (2021), 118327, https://doi.org/10.1016/j.seppur.2021.118327.
[271] S. Xin, S. Huo, C. Zhang, X. Ma, W. Liu, Y. Xin, et al., Coupling nitrogen/oxygen self-doped biomass porous carbon cathode catalyst with $CuFeO_2$/biochar particle catalyst for the heterogeneous visible-light driven photo-electro-Fenton degradation of tetracycline, Appl Catal B 305 (2022), 121024, https://doi.org/10.1016/j.apcatb.2021.121024.
[272] S. Zhu, W. Wang, Y. Xu, Z. Zhu, Z. Liu, F. Cui, Iron sludge-derived magnetic Fe_0/Fe_3C catalyst for oxidation of ciprofloxacin via peroxymonosulfate activation, Chem Eng J 365 (2019) 99–110, https://doi.org/10.1016/j.cej.2019.02.011.
[273] F. Rahimi, J.P. van der Hoek, S. Royer, A. Javid, A. Mashayekh-Salehi, M. Jafari Sani, Pyrite nanoparticles derived from mine waste as efficient catalyst for the activation of persulfates for degradation of tetracycline, J Water Process Eng 40 (2021), 101808, https://doi.org/10.1016/j.jwpe.2020.101808.
[274] L. He, M.X. Li, F. Chen, S.S. Yang, J. Ding, L. Ding, et al., Novel coagulation waste-based Fe-containing carbonaceous catalyst as peroxymonosulfate activator for pollutants degradation: role of ROS and electron transfer pathway, J Hazard Mater 417 (2021), 126113, https://doi.org/10.1016/j.jhazmat.2021.126113.
[275] S. Zhu, Y. Xu, Z. Zhu, Z. Liu, W. Wang, Activation of peroxymonosulfate by magnetic Co-Fe/SiO_2 layered catalyst derived from iron sludge for ciprofloxacin degradation, Chem Eng J 384 (2020), 123298, https://doi.org/10.1016/j.cej.2019.123298.
[276] M. Li, F. Huang, L. Hu, W. Sun, E. Li, D. Xiong, et al., Efficient activation of peroxymonosulfate by a novel catalyst prepared directly from electrolytic manganese slag for degradation of recalcitrant organic pollutes, Chem Eng J 401 (2020), 126085, https://doi.org/10.1016/j.cej.2020.126085.

[277] Y. Zhao, H. Wang, X. Li, X. Yuan, L. Jiang, X. Chen, Recovery of CuO/C catalyst from spent anode material in battery to activate peroxymonosulfate for refractory organic contaminants degradation, J Hazard Mater 420 (2021), 126552, https://doi.org/10.1016/j.jhazmat.2021.126552.
[278] H. Liu, Y. Liu, L. Tang, J. Wang, J. Yu, H. Zhang, et al., Egg shell biochar-based green catalysts for the removal of organic pollutants by activating persulfate, Sci Total Environ 745 (2020), 141095, https://doi.org/10.1016/j.scitotenv.2020.141095.
[279] M.M. Mian, G. Liu, Activation of peroxymonosulfate by chemically modified sludge biochar for the removal of organic pollutants: understanding the role of active sites and mechanism, Chem Eng J 392 (2020), 123681, https://doi.org/10.1016/j.cej.2019.123681.
[280] W. Wang, M. Chen, Catalytic degradation of sulfamethoxazole by peroxymonosulfate activation system composed of nitrogen-doped biochar from pomelo peel: important roles of defects and nitrogen, and detoxification of intermediates, J Colloid Interface Sci 613 (2022) 57–70, https://doi.org/10.1016/j.jcis.2022.01.006.
[281] Y. Hu, D. Chen, R. Zhang, Y. Ding, Z. Ren, M. Fu, et al., Singlet oxygen-dominated activation of peroxymonosulfate by passion fruit shell derived biochar for catalytic degradation of tetracycline through a non-radical oxidation pathway, J Hazard Mater 419 (2021), 126495, https://doi.org/10.1016/j.jhazmat.2021.126495.
[282] G. Geng, Y. Gao, Z. Zhang, K. Gao, W. Zhang, J. Song, Renewable and robust biomass waste-derived Co-doped carbon aerogels for PMS activation: catalytic mechanisms and phytotoxicity assessment, Ecotoxicol Environ Saf 220 (2021), 112381, https://doi.org/10.1016/j.ecoenv.2021.112381.
[283] J. Wang, Z. Liao, J. Ifthikar, L. Shi, Y. Du, J. Zhu, et al., Treatment of refractory contaminants by sludge-derived biochar/persulfate system via both adsorption and advanced oxidation process, Chemosphere 185 (2017) 754–763, https://doi.org/10.1016/j.chemosphere.2017.07.084.
[284] J. Zhu, Y. Song, L. Wang, Z. Zhang, J. Gao, D.C.W. Tsang, et al., Green remediation of benzene contaminated groundwater using persulfate activated by biochar composite loaded with iron sulfide minerals, Chem Eng J 429 (2022), 132292, https://doi.org/10.1016/j.cej.2021.132292.
[285] J. Wang, M. Shen, Q. Gong, X. Wang, J. Cai, S. Wang, et al., One-step preparation of ZVI-sludge derived biochar without external source of iron and its application on persulfate activation, Sci Total Environ 714 (2020), 136728, https://doi.org/10.1016/j.scitotenv.2020.136728.
[286] Y. Gao, Q. Zhao, Y. Li, Y. Li, J. Gou, X. Cheng, Degradation of sulfamethoxazole by peroxymonosulfate activated by waste eggshell supported Ag_2O-Ag nano–particles, Chem Eng J 405 (2021), 126719, https://doi.org/10.1016/j.cej.2020.126719.
[287] M. Li, D. Xia, H. Xu, Z. Guan, D. Li, Iron oxychloride composite sludge-derived biochar for efficient activation of peroxymonosulfate to degrade organic pollutants in wastewater, J Clean Prod 329 (2021), 129656, https://doi.org/10.1016/j.jclepro.2021.129656.